1989

Establishment of a capability to measure optical transition radiation

Dallman, Peter Karl

Monterey, California. Naval Postgraduate School

NAVAL POSTGRADUATE SCHOOL
Monterey, California

THESIS

ESTABLISHMENT OF A CAPABILITY TO MEASURE OPTICAL TRANSITION RADIATION

by

Peter Karl Dallman

December 1989

Thesis Advisor: X. K. Maruyama

REPORT SECURITY CLASSIFICATION Unclassified	1b RESTRICTIVE MARKINGS
SECURITY CLASSIFICATION AUTHORITY	3 DISTRIBUTION/AVAILABILITY OF REPORT Approved for public release; distribution is unlimited.
DECLASSIFICATION/DOWNGRADING SCHEDULE	
PERFORMING ORGANIZATION REPORT NUMBER(S)	5 MONITORING ORGANIZATION REPORT NUMBER(S)
NAME OF PERFORMING ORGANIZATION Naval Postgraduate School 6b OFFICE SYMBOL (*If applicable*) 33	7a NAME OF MONITORING ORGANIZATION Naval Postgraduate School
ADDRESS (*City, State, and ZIP Code*) Monterey, CA 93943-5000	7b ADDRESS (*City, State, and ZIP Code*) Monterey, CA 93943-5000
NAME OF FUNDING/SPONSORING ORGANIZATION 8b OFFICE SYMBOL (*If applicable*)	9 PROCUREMENT INSTRUMENT IDENTIFICATION NUMBER
ADDRESS (*City, State, and ZIP Code*)	10 SOURCE OF FUNDING NUMBERS PROGRAM ELEMENT NO. / PROJECT NO / TASK NO / WORK UNIT ACCESSION NO

TITLE (*Include Security Classification*) ESTABLISHMENT OF A CAPABILITY TO MEASURE OPTICAL TRANSITION RADIATION

PERSONAL AUTHOR(S) Dallman, Peter, K.

TYPE OF REPORT	13b TIME COVERED	14 DATE OF REPORT (*Year, Month, Day*)	15 PAGE COUNT
Master's Thesis	FROM _____ TO _____	December 1989	103

SUPPLEMENTARY NOTATION The views expressed in this thesis are those of the author and do not reflect the official policy or position of the Department of Defense or the U.S. Government

COSATI CODES		
FIELD	GROUP	SUB-GROUP

18 SUBJECT TERMS (*Continue on reverse if necessary and identify by block number*)
optical transition radiation, charged particle beams, beam profiling

ABSTRACT (*Continue on reverse if necessary and identify by block number*)

Optical transition radiation (OTR) can be used as a beam diagnostic system for charged particle beams. The experimental setup developed here demonstrates the capability to observe and measure OTR due to an electron beam from a linear accelerator. The setup is compact, simple, and readily adapted to experimental work. Through the use of two software programs (QuickCapture and Image 1.14) and the QuickCapture frame grabber board, both qualitative and quantitative results are possible. One of the useful qualitative results is a three-dimensional beam profile, which is quickly produced from a captured image. The system measured the relative intensity with a 3% variation between several images of the same source. Angular measurements of OTR can be made with an angular resolution of 600 microradians.

DISTRIBUTION/AVAILABILITY OF ABSTRACT ☒ UNCLASSIFIED/UNLIMITED ☐ SAME AS RPT ☐ DTIC USERS	21 ABSTRACT SECURITY CLASSIFICATION Unclassified
NAME OF RESPONSIBLE INDIVIDUAL X.K. Maruyama	22b TELEPHONE (*Include Area Code*) (408) 646-2431 22c OFFICE SYMBOL 61Mx

DD FORM 1473, 84 MAR 83 APR edition may be used until exhausted. All other editions are obsolete

SECURITY CLASSIFICATION OF THIS PAGE

☆ U.S. Government Printing Office 1986—606-243

Unclassified

Approved for public release; distribution is unlimited

Establishment of a Capability to Measure Optical Transition Radiation

by

Peter K. Dallman
Lieutenant, United States Navy
B.S., United States Naval Academy, 1984

Submitted in partial fulfillment of the
requirements for the degree of

MASTER OF SCIENCE IN PHYSICS

from the

NAVAL POSTGRADUATE SCHOOL
December 1989

ABSTRACT

Optical transition radiation (OTR) can be used as a beam diagnostic system for charged particle beams. The experimental setup developed here demonstrates the capability to observe and measure OTR due to an electron beam from a linear accelerator. The setup is compact, simple, and readily adapted to experimental work. Through the use of two software programs (QuickCapture and Image 1.14) and the QuickCapture frame grabber board, both qualitative and quantitative results are possible. One of the useful qualitative results is a three-dimensional beam profile, which is quickly produced from a captured image. The system measured the relative intensity with a 3% variation between several images of the same source. Angular measurements of OTR can be made with an angular resolution of 600 microradians.

TABLE OF CONTENTS

ACKNOWLEDGEMENTS

I would like to thank Dr. Ralph Fiorito, whose ideas are prominent throughout this work, and Dr. Don Rule for his assistance. I am grateful for the enthusiasm, optimism and guidance of my thesis adviser, Dr. Xavier Maruyama.

As in any experimental work, much "hands-on" experience is learned from the technicians who make things happen. My thanks goes to Mr. Don Snyder and Mr. Harold Riedtyk who answered my questions even after things were broken.

I would also like to thank Lieutenant Dave Caldwell for many hours spent assisting this work.

Finally and foremost, I thank my wife, Michelee, for her encouragement and support. In appreciation, this work is dedicated to her.

I. INTRODUCTION

A. PURPOSE OF EXPERIMENT

Optical transition radiation, or OTR, occurs when a charged particle crosses the interface between two media with different dielectric constants. OTR was predicted in 1944 by Frank and Ginsburg [Ref. 1]. Much work has been done by others to illustrate the utility of applying OTR as a real-time diagnostic system for charged particle beams [Refs. 2-10]. Sustained interest in particle beam applications has created the need for diagnostic systems which are compact, real-time, and easily adapted to experimental work. The purpose of this experiment was to establish the capability to observe and measure optical transition radiation with these diagnostic system features in mind.

B. THE PHENOMENON OF OPTICAL TRANSITION RADIATION

Although a more detailed description of OTR theory can be found in Appendix A, a short overview of the phenomenon of OTR will be presented here. As a charged particle moves from one medium to another medium with a different dielectric constant, transition radiation occurs. A wide spectrum of frequencies are produced, including optical frequencies, so OTR can be viewed with standard optical equipment such as video cameras. Optical transition radiation patterns appear

cone-shaped in three dimensions, and V-shaped in two dimensions. Figure 1 shows the forward and backward radiation cones produced at normal incidence and at oblique incidence. Normal incidence does not allow the experimentalist to view the OTR pattern since both the forward and backward cones are centered about the electron beam path. Oblique incidence reflects the backward OTR pattern away from the electron beam path, allowing one to view transition radiation. The backward OTR pattern is centered about the angle of specular reflection, i.e., the angle of reflection from a mirror or polished metal surface used as a reflector. Centered at the angle of specular reflection are a focusing lens and a TV camera for the purposes of viewing OTR patterns.

C. OVERVIEW OF EXPERIMENT

The experiment was performed on the linear accelerator (LINAC) located at the Naval Postgraduate School (NPS), Monterey, California. In the experimental setup, a laser beam is used to align optical components which view the OTR pattern. Originally, the laser beam would have been an alignment aid, and the electron beam would have been the measured parameter of interest. Unfortunately, on October 17, 1989, a significant earthquake of magnitude 7.1 caused damage to many areas in northern California, including the LINAC at the Naval Postgraduate School. (Approximately 30

OPTICAL TRANSITION RADIATION PATTERNS

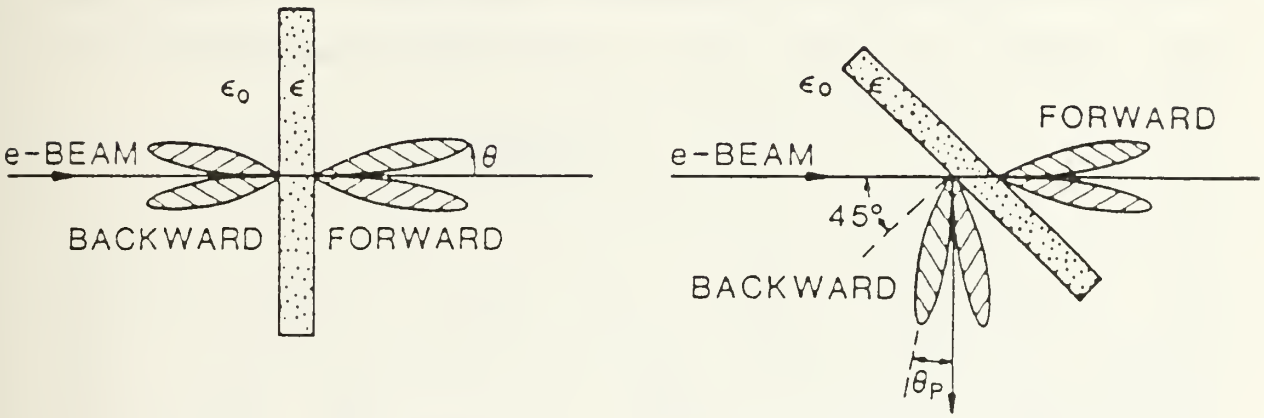

Figure 1: The optical transition radiation patterns produced by normal and oblique incidence. Normal incidence does not allow viewing because the radiation pattern is centered around the electron beam. Oblique incidence reflects the backward OTR pattern away from the electron beam so that it can be viewed. ε and ε_0 are the dielectric constants for the medium and vacuum, respectively. [Ref. 5]

minutes before the earthquake struck, OTR was observed at the NPS LINAC; this was the first time OTR was observed with the experimental setup described in Chapter II.) In light of this completely unforeseen misfortune, the capability to measure OTR was developed using the light from a target illuminated by a laser beam instead of using the OTR light produced by an electron beam. Since a laser beam can be filtered and measured in much the same way as an actual OTR beam image, this work uses a laser beam to establish a capability to measure optical transition radiation.

In addition to the OTR pattern, the setup permits focusing on the beam spot as it hits the OTR foil. A small power laser beam is used in an alignment procedure which couples the laser beam and the electron beam. The coincidence of the two beams provides the ability to calibrate measurements.

Live images of the OTR pattern are taken with a TV camera which is linked with a computer. A frame-grabber board is added to the computer hardware and allows still video images to be taken from the live video input. Images are stored in a digitized format. Software programs designed specifically for digital image processing and analysis have been installed on the computer. The procedure for capturing images from live video is discussed. Several other software functions are also investigated in detail, such as one dimensional line

scans, three dimensional profile plots, integrated density, frame averaging, and filtering.

A calibration procedure called a lens scan is detailed. TV camera response is examined, along with methods to reduce background noise. The effect of different orientations and positions of neutral density filters in the beam path is considered. Finally, a capability to measure relative intensity is mentioned.

D. POTENTIAL APPLICATION

As mentioned, continued interest in the area of high energy charged particle beam physics is expected. This implies a need to develop particle beam diagnostic systems which are simple to use, compact, real-time, and easily adapted to experimental work. The setup described in this thesis meets those criteria. An OTR beam profile monitoring system would have certain advantages over a system such as the Bates fast wire beam scanner, currently under development at the Massachusetts Institute of Technology. The Bates system uses a rather complicated system which moves a thin wire through the electron beam path in about ten seconds. Secondary emissions from the wire as a function of the wire position determine the electron beam profile. After the signal is digitized, it is processed via a microcomputer and a microvax computer to provide real time beam profiles.

Although this system has great potential, it requires its own dedicated microvax computer, needs periodic recalibration, takes several seconds to produce a beam profile, and is a complicated, intricate design. [Ref 11]

The OTR beam profile measuring system described in this thesis requires only a microcomputer, needs no recalibration, produces instant beam profiles, and is a relatively simple design. It is possible that OTR could be used as an alternative to the Bates fast wire beam scanner in providing a useful beam diagnostic system.

II. EXPERIMENTAL SETUP AND PROCEDURE

A. EQUIPMENT SETUP

This experiment was performed using the linear electron accelerator at the Naval Postgraduate School in Monterey, California. Appendix B lists LINAC characteristics and a schematic of the layout. The LINAC area is divided into two sections: the target area and the control room.

1. Target Area

The target area contains several optical components mounted on an optical breadboard, and also some optical components inside the vacuum line of the LINAC. The optical breadboard is placed next to the electron beam line. This experimental design contains optical components which are low in overall height, and requires only about 30 centimeters of clearance between the surface of the optical breadboard and the electron beam.

The underlying philosophy of this setup is to fully align the optical components using a laser, and then to couple the entire optical setup to the electron beam. Although this alignment and coupling process is a tedious task, electron beam time is saved since most of the alignment is completed beforehand.

Figure 2 shows the experimental setup. A low power laser is the first main optical component, and it is used to align the other optical components with the linear accelerator and OTR foil. A post type laser mount was used, which has a vertical control and steering alignment control in the horizontal plane.

Neutral density filters are placed in front of the laser to reduce the intensity in order to prevent damage to the TV camera. The light from the laser then enters the vacuum line of the LINAC through a viewport, reflecting off a retractable alignment mirror in the large chamber. The alignment mirror is oriented at 45^{o} to the electron beam and also the laser beam. A fluorescent view-screen is placed on the back of the mirror so that the electron beam can be directed to the same point on the mirror as the laser beam. This establishes the first of two points in space which define the line of the electron beam and the laser beam. The mirror is mounted on a holder assembly with tilt control for alignment purposes, and the mount is attached to a linear motion vacuum feedthrough so that the mirror can be removed from the electron beam line.

Downbeam from the retractable mirror is the OTR foil holder mounted inside a six-way vacuum cross. The foil holder has two miniature rotary motion vacuum feedthroughs which control the tilt of the foil through a custom-made

Experimental Setup in Target Area

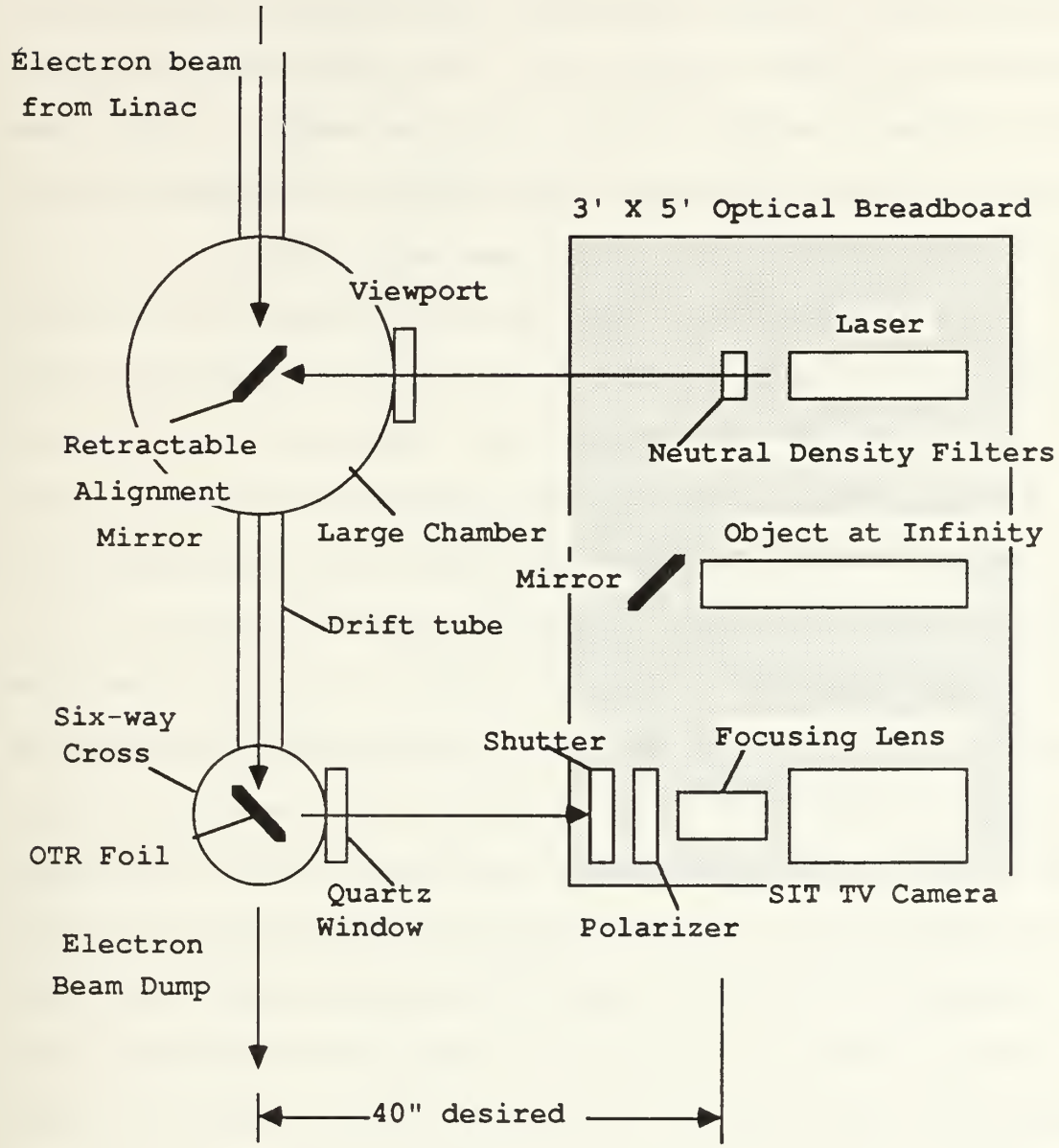

Figure 2: Target area setup. In order to achieve collinearity, the laser beam and electron beam are focused onto two points: the retractable alignment mirror and the TV camera.

mount. Since the OTR foil holder is oriented at 45° to the electron beam, backward OTR light comes off the foils at 90° to the electron beam line. The light then passes through a quartz window, a shutter, and a polarizer before entering the focusing lens and TV camera. (The OTR foil could actually be a reflective metallic foil or a front surface mirror.)

The particular focusing lens chosen was a 200 millimeter Canon lens, with a focal distance of f/1:2.8. The mount for the lens includes two separate single axis translation stages. One stage is manually controlled and oriented perpendicular to the beam, and the other stage is a remotely controlled, motorized stage with a two inch travel, and is oriented with the beam path. Directly above the translation stages are a 360 degree rotary stage which allows horizontal rotation of the lens, and a dual axis tilt table which allows tilting out of the horizontal plane. The camera lens is mounted on a post centered in the middle of both the rotary stage and the tilt table. This centering of the lens and direct coupling of the rotary stage and tilt table are necessary to align the camera lens with the center of the OTR pattern.

Immediately after going through the focusing lens, the OTR light enters the TV camera. Since OTR produces light patterns that are not very intense, the TV camera must be sensitive to low light levels. In order to understand the

limitations of the TV camera, two types were used: a silicon intensified target TV camera (SITCAM) designed for low light level applications, and a vidicon used in everyday applications. The mount for the TV camera consists of an optical laboratory jack for vertical control, and a dual axis translation stage for control in the horizontal plane. Because the electron beam and laser beam can be focused onto the same point on the TV camera, the second alignment point is established. Collinearity between the two beams is achieved by matching the two alignment points: one on the retractable alignment mirror, the other on the TV camera.

An additional optical element on the optical breadboard is the "object at infinity," shown in Figure 3. The phrase object at infinity implies parallel light and this is precisely how this element works. A light source is converted into a point light source by putting it directly behind an iris diaphragm that is almost completely closed. The point light source passes over a sector star target (a common focusing device shown in Figure 4). Behind the sector star target is a plano convex lens. The distance between these two components equals the focal length of the lens, namely 100 millimeters. Since the object light coming into the lens is at the focal distance, the image is at infinity, or in other words, the light emerging from the lens is parallel light. A mirror then reflects the parallel light

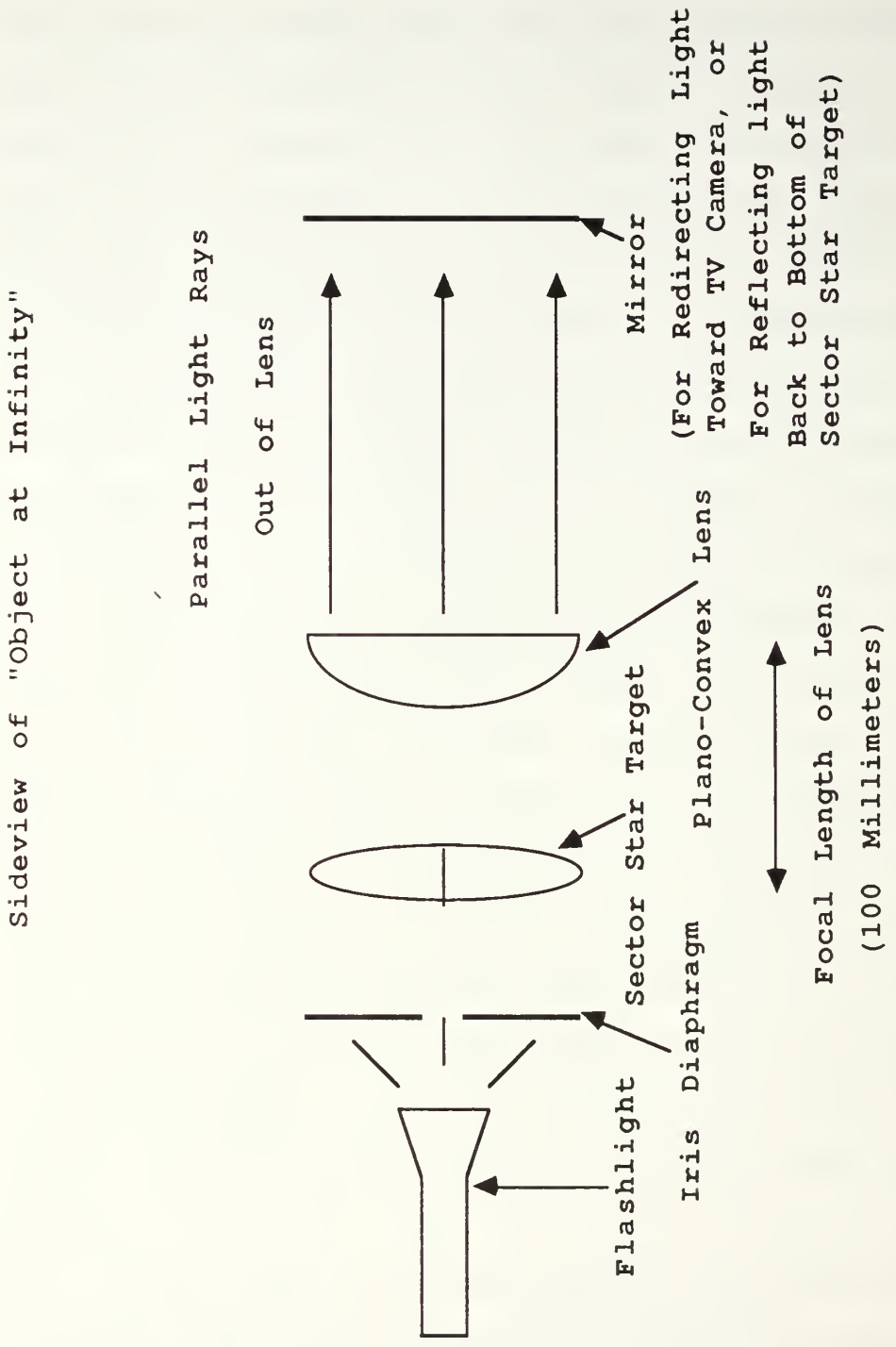

Figure 3: Sideview of "object at infinity". The point light illuminates the sector star target which is at the focal distance of the lens. Parallel light is emitted from the lens.

Figure 4: Sector star target. This is a focusing device used to produce the "object at infinity." The bottom half is covered so that the image can be reflected off a mirror and back on to the lower half of the target.

either back onto the bottom side of the sector star for the purpose of focusing the lens, or reflects the light on toward the lens and TV camera to give the "object at infinity."

2. Control Room

As shown in Appendix B, the control room is located several meters away from the target area near the front end of the accelerator. The control room contains the computer and video monitoring equipment which remotely control the experimental setup. The video signal from the TV camera in the target area is sent via a braided cable to the control room, where it is monitored and processed. A schematic of the control room setup is shown in Figure 5.

First, the video signal is digitized by a digitizer which is linked to a camera control unit for remote operation of the camera. This digital signal then goes to a Macintosh II PC via an EP205 jumper cable. The jumper cable feeds into the DT2255-60 Hz QuickCapture frame grabber board which is installed directly into an expansion board slot in the back of the Macintosh II PC. The frame grabber board captures a digital picture from the incoming video signal and stores it in the computer.

Two software packages were used to process and analyze the digital images obtained by the frame grabber board. QuickCapture has its own software program and has a limited capability. Image Version 1.14 is the other software program

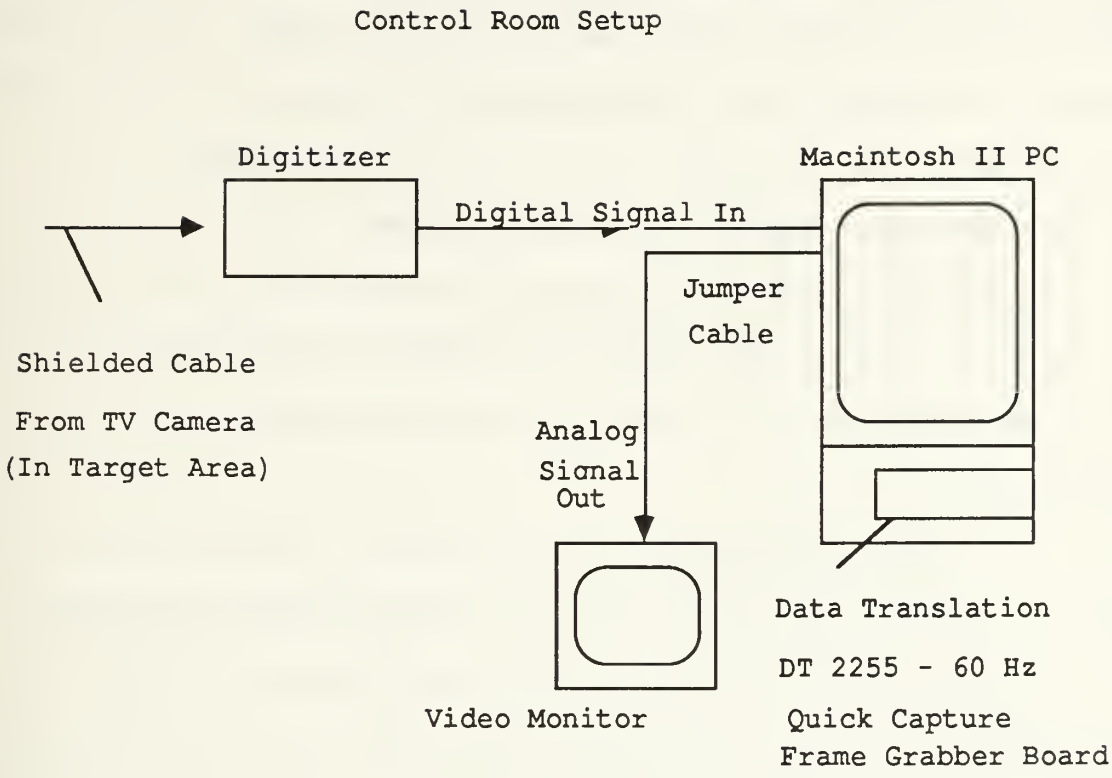

Figure 5: Control room setup. Video signal enters Macintosh II PC and is captured by frame grabber board in digitized format.

which was used and has great utility for the purposes of OTR. Both of these software packages will be discussed in detail at the end of this chapter.

Also in the control area is a video monitor which is fed an analog signal from the Macintosh II PC. This extra monitor is helpful for viewing the TV camera's output when the Macintosh II PC is not in the "live video" mode.

3. Optical Design Considerations

Because optical transition radiation is an optical phenomenon, there are several design considerations which will be explained in order to understand the experimental setup used.

A main feature of the optical setup is the 200 millimeter lens which is used to focus between the object at infinity and the OTR foil. Since the translation stage which holds this lens can only travel 5 centimeters (2 inches), one needs to calculate the distance between the OTR foil and the lens to ensure that proper focusing is possible. One can define r_o as the object distance (from foil to lens), r_i as the image distance (from lens to image plane), and N as the number of focal lengths, such that $r_o = Nf$. In this case, f = 20.1 centimeters = 7.9 inches. Since the maximum travel of the translation stage is 5 centimeters (two inches), $r_i - f$ = 5.0 cm, and r_i = 25.1 cm. Recalling the Gaussian lens formula [Ref 12],

$$\frac{1}{f} = \frac{1}{r_o} + \frac{1}{r_i} ,$$

one can determine r_o by letting $r_o = Nf$ where f is the focal length of the lens. Solving first for N, cross-multiplying gives

$$r_i r_o = r_i f + r_o f ,$$

and substituting for r_o where $r_o = nf$ gives

$$N [f r_i - f^2] = r_i f ,$$

which can be solved for N:

$$N = \frac{r_i}{r_i - f} = \frac{25.1}{5.0} = 4.92 .$$

Similarly, one can solve the Gaussian lens formula for r_o where

$$r_o = r_i(N-1) = 99.3 \text{ cm.}$$

This means that in order for the travel of the lens to be 5 centimeters or less, the lens can come no closer to the OTR foil than 99.3 centimeters. In the same manner, it can be shown that for 3.8 centimeters (1.5 inches) of lens travel, the separation distance will be 1.26 meters. Therefore,

there is a minimum distance of about 1 meter from the OTR mirror to the focusing lens, but this can be larger.

As can be seen from the above calculation, a focal length of 200 millimeters was used for the focusing lens. The reason for choosing a focal length of 200 millimeters was limited by the length of travel of the translation stage which was 5 centimeters. Longer travel translation stages are not readily available. A different focal length lens could have been used, but the geometry of the setup suggests a focal length of this order.

Another noteworthy dimension in the optical setup is the distance between the retractable alignment mirror and the OTR foil. This distance was chosen to be at least one meter for the reason that over 1 meter, a 1 milliradian angle corresponds to 1 millimeter of distance perependicular to the beam line. Of course, smaller measurements than one millimeter are achievable when seen on the TV camera where individual pixel positions are distinguishable.

B. PROCEDURE

1. Alignment

Optical transition radiation is a highly directional phenomena, and produces a light cone centered around the angle of specular reflection, with a maximum intensity at an angle of $1/(\gamma)$ from specular reflection (γ is the Lorentz factor). Energies of interest are in the tens of MeV range,

so the light cone produced is of the order of a few milliradians. A critical alignment procedure is required to get meaningful measurements. The alignment process is time consuming, but is straightforward to describe. By referring to the experimental setup in the target area shown in Figure 2, the following alignment procedure can be understood.

The laser is used to align the optical equipment, and this setup is coupled to the electron beam. Since two points in space define a line, forcing the laser light and the electron beam through the same two points achieves collinearity. The first point is in the center of the retractable alignment mirror in the first vacuum chamber. The second point is on the TV camera, where the OTR light and the laser light can both be viewed.

A necessary first step is to level the optical breadboard using a carpenter's level. Then, each component is aligned sequentially without adjusting what has been aligned before it. The basic technique is to use a series of centering and retro-reflections to put the laser light in the geometrical center of its path. The retro-reflections ensure that the laser light is normal to the surface it hits.

The laser is centered and retro-reflected off the small viewport window where the laser light enters the large chamber. Next, the light hits the retractable alignment mirror. This mirror is actually a glass plate with a

half-silvered front so the laser light can reflect off it. A fluorescent screen is centered on the back with a cross-hair on it and hole in its center. The screen is positioned so that the laser light goes through its center, and then the electron beam can be steered through the center of the screen also. Thus, the first alignment point is established.

The retractable alignment mirror must then be positioned so that the laser light goes down the center of the drift tube between the large chamber and the six-way cross. A fiducial (plexiglass disc with the center marked) was placed inside the exit point of the large chamber. The alignment mirror was adjusted until the laser light reflecting off it was centered on the fiducial, and also on the beam dump window of the six-way cross. Once this is done, the OTR foil holder assembly can be installed in the six-way cross. The OTR foil holder is positioned so that the laser light reflecting off it is in the center of the quartz viewport exit window. The laser light should be the same height above the optical table as it was before it entered the vacuum line.

The next step is to align the optical rail which holds the lens and TV camera. The optical rail is aligned to the laser beam by putting an object on the rail, such as the camera lens mount, and sliding it between the near and far ends of the optical rail until the laser spot does not move

on the object. After the optical rail is aligned, the TV camera is aligned by centering on its cover plate and retro-reflecting back to the quartz window. Similarly, the camera lens is aligned by centering and retro-reflecting on a lens cap with its center marked. The lens mount has enough degrees of freedom, so that this is not a difficult task.

As outlined in this procedure, the laser light should appear in the center of the TV camera's picture. To ensure that the laser spot is centered, one can turn the TV camera on and look at live video. Moving the TV camera horizontally or vertically will center the laser spot.

2. Focusing

Because of the particular nature of optical transition radiation patterns, there are two focal points of interest. Figure 6 shows the two focal points which will be described.

The parallel light from an OTR pattern is focused at the focal plane of the focusing lens. The parallel light source for this half of the focusing procedure is the object at infinity. The image seen at the focal plane of the lens is the OTR pattern of concentric circles. A one dimensional intensity scan of this image will produce the characteristic double hump of OTR.

The other focal point of interest is at the beam spot on the OTR foil itself. At this image plane, the beam

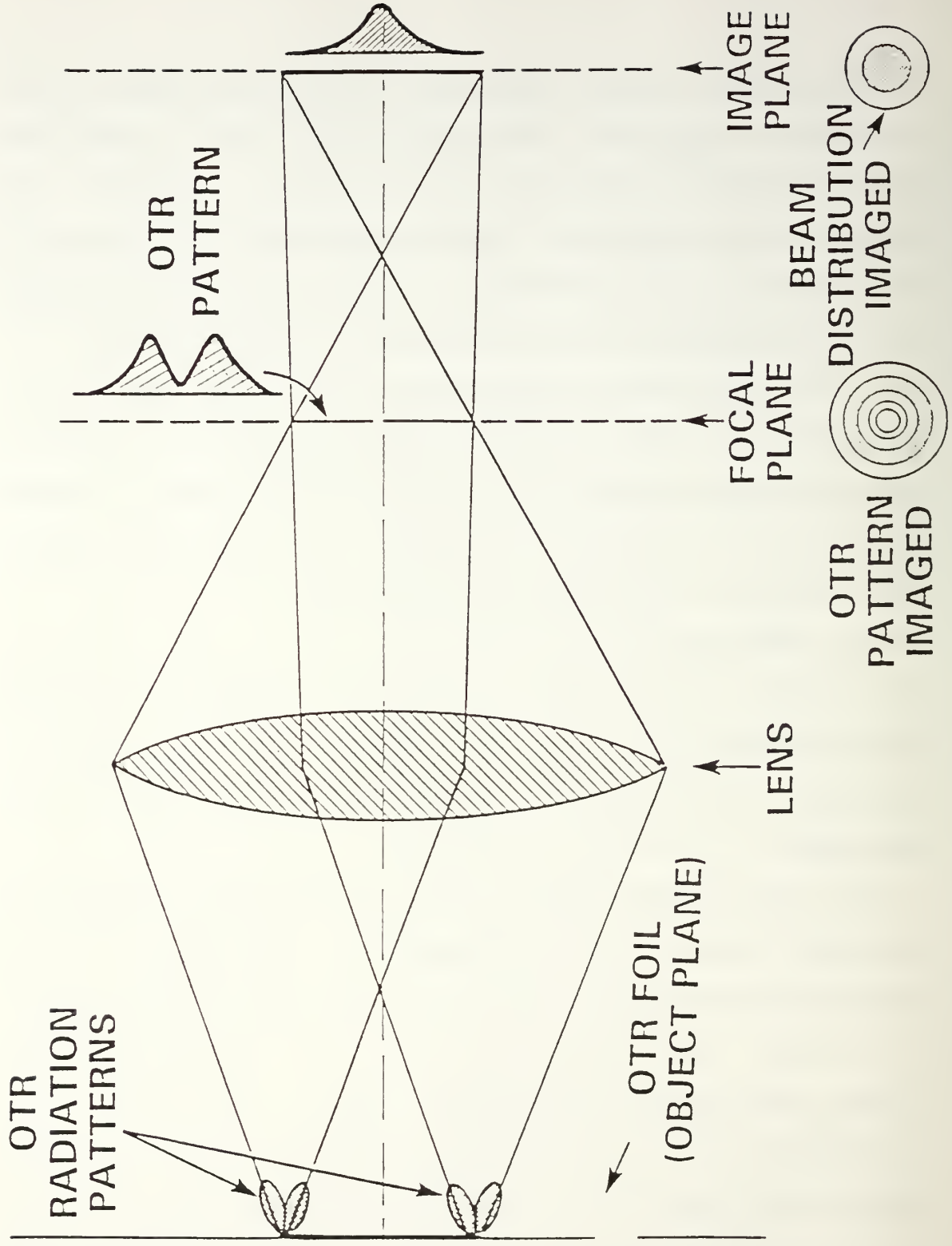

Figure 6: Optical ray diagram for OTR. Note two diffrerent focal planes give two different images. [Ref. 13]

distribution will be visible. A one dimensional intensity scan of this image will produce a profile of the beam intensity.

The method of focusing at the two focal points just described will be outlined below.

It should be noted that in this experimental setup, the focusing lens is moved to produce the desired image. The plane where the image is produced, i.e., the TV camera is not moved. A small movement of the focusing lens gives two different images. Both images provide useful imformation.

Focusing at the two focal points is easily accomplished because the focusing lens is mounted on a remotely controlled, motorized translation stage. The first point at which to focus the lens is the object at infinity. The light from the object at infinity can be redirected with two mirrors on posts to go into the focusing lens and TV camera. This will give the sector star target pattern. Once this focus point is found, the position is noted on the digital readout of the controller for the translation stage. The setup shown below in Figure 7 shows how the focusing is done. (Note that this setup is only a slight modification from the experimental setup shown before in Figure 2.)

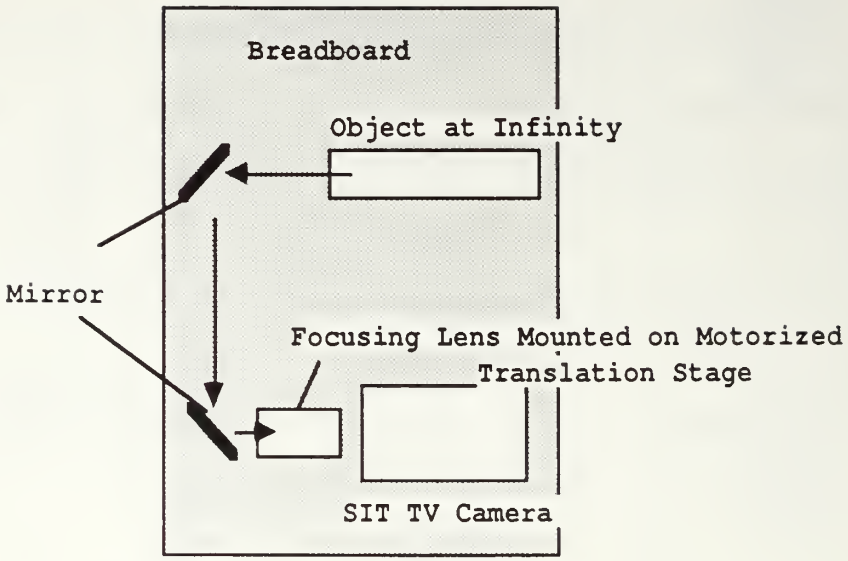

Figure 7: Focusing on the object at infinity. The object at infinity (shown previously in Figure 3) produces parallel light rays. This parallel light is reflected into the focusing lens to establish one of the two focal points for the lens.

The other focal point is the beam spot on the surface of the OTR foil itself. The smooth surface of the OTR foil provides no object on which to focus. Another object can be placed at the same distance from the lens as the OTR foil, and focusing can be accomplished on it instead. A sketch is shown below in Figure 8. Thus, the two focusing positions are established. Focusing at infinity gives the OTR pattern, which is the characteristic double hunp in one dimension. Focusing at the OTR foil yields the beam profile.

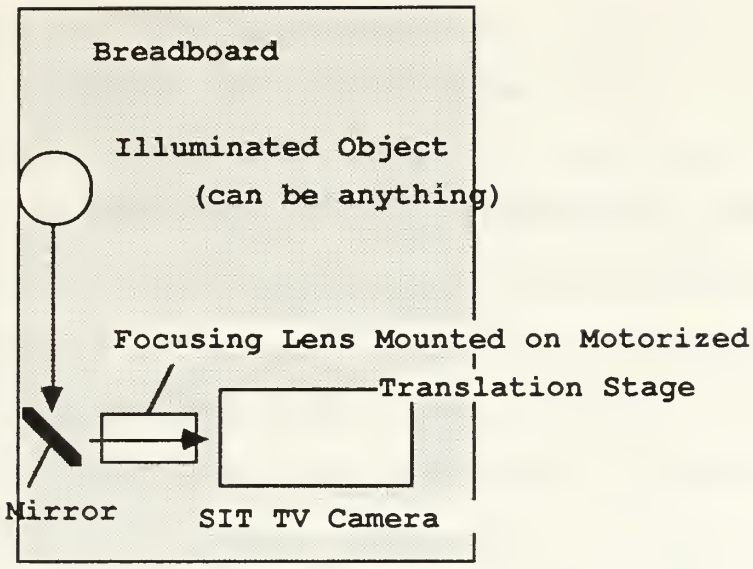

Figure 8: Focusing on the beam spot. The distance from the focusing lens to the illuminated object equals the distance from the focusing lens to the OTR foil.

Once the focusing at the two positions has been accomplished, the optical preparations are complete. The experiment can proceed by running the linear accelerator. The electron beam is focused onto the two points established by the laser beam: the center of the alignment mirror in the first chamber (which can be viewed through a window with an extra TV camera), and the center of the main TV camera picture. Coupling the laser beam and electron beam is an iterative process since only one point can be established at a time.

III. UNDERSTANDING THE SOFTWARE

A. GENERAL DESCRIPTION OF THE SOFTWARE

Chapter II described an experimental setup and procedure which generates a video image of an optical transition radiation pattern. The video image is input into a microcomputer for image processing and analysis; a Macintosh II PC was used in this work. Video image processing and analysis were accomplished through the use of two software programs. The QuickCapture software application provided along with the QuickCapture frame grabber board has a somewhat limited image processing capability. Image Version 1.14 is a public domain shareware program designed by the National Institute of Health, Bethesda, Maryland. Image 1.14 has an excellent capability to process digital images. Both of these programs will be discussed in detail in this chapter.

1. QuickCapture

The QuickCapture software package complements the Quickcapture frame grabber board mentioned earlier. Both are manufactured by Data Translation, Inc., of Marlboro, Massachusetts. Together, the frame grabber board and QuickCapture application allow the user to capture images in digital format from the live video signal it receives. An outline of some of QuickCapture's menus and functions is

shown in Table 1. The program accepts color or black and white images in analog or digital format, and offers up to 256 possible gray levels on a 480 by 640 pixel picture. QuickCapture has the capability to capture images, display live video, sharpen and smooth images, and perform arithmetic operations between two images. Subtraction of one image from another is one of the available arithmetic operations. The subtraction function can be used to subtract a blank background image from an image which has a beam spot on it, a process which is of interest when analyzing beam profiles, such as in OTR patterns. [Ref. 14]

2. Image Version 1.14

Image Version 1.14 was the main software package used in this experiment for image processing and analysis. Image 1.14 is a public domain program designed specifically for digital image processing and analysis on a Macintosh II PC. Designed by the National Institute of Health in Bethesda, Maryland, the program can acquire, enhance, measure, edit, animate, and print images. Table 2 lists an outline of some of the functions that are possible with this program. Not listed on Table 2 are the functions previously listed in Table 1; Image 1.14 can perform all the functions offered by the QuickCapture program.

The Image 1.14 program supports the Data Translation QuickCapture frame grabber board for digitizing images using

MENU NAME, Function

IMAGE MENU

Capture - captures an image.

Live video - displays live video image.

Statistics - shows the distribution of gray levels in a selected area.

GRAYSCALE MENU

Several options available wich allow user to choose 2, 16, 64, or 256 gray levels in the displayed image.

ENHANCE MENU

Sharpen - increases contrast in selected areas.

Smooth - decreases contrast in selected areas.

Histogram Equalization - evenly distributes the grayscale values of the pixels in a selected area.

Image Calculator - performs arithmetic functions

Addition/Subtraction - will add/subtract two images, or to add/subtract a constant value to an image.

Multiplication/Division - will multiply/divide by a constant to increase/reduce contrast.

TABLE 1: Some of the QuickCapture options available to user.

MENU NAME, Function

FILE MENU

Import - allows user to import image files created by non-Macintosh systems.

FUNCTIONS MENU

Filtering - 3 x 3 spatial convolutions allow the user to Smooth, Sharpen, Convolve, Reduce Noise and Convolve.

Average Frames - user specifies number of frames to be averaged. Requires large amount of computer memory.

ANALYSIS MENU

Measure - computes the area, mean, standard deviation, minimum and maximum intensity, perimeter length and integrated density of selected area.

Column Average Plot - provides density profile of selected rectangular area.

3D Plot - generates a 3D display of the current selection.

Save Blank Field - used to correct for nonuniform camera response.

TOOL (Tools are found under Look-Up Table)

Density Profile Tool - provides a one dimensional intensity line scan selected by user. Line can be 1, 2, 3, 4, 6, or 8 pixels in width.

TABLE 2: Some of Image 1.14's options. All of QuickCapture's options are also available, but are not listed here.

a TV camera. Like QuickCapture, Image 1.14 also accepts either color or black and white images in digital format. It displays 256 color or shades of gray, and creates images that are 512 pixels high by 600 pixels wide. The program imports and exports files in both the TIFF and PICT format, providing compatibility with many other Macintosh applications. (TIFF and PICT are just two of several different file formats. TIFF is a good format for saving digital images, while PICT is useful for images to be exported to other Macintosh applications.) Standard image processing functions include histogram equalization, density profiling, smoothing, sharpening, noise reduction, spatial convolutions, and a variety of measurement functions. Acquired images can be frame averaged, shading corrected, and magnified up to eight times. Image 1.14 is easy to learn and is ideally suited for image processing associated with optical transition radiation experiments.

B. MASTERING THE SOFTWARE

Having described the general features of the two software programs, specific procedures for capturing, processing, and analyzing video images will now be discussed. Because Image 1.14 has image processing capabilities in addition to the same basic functions as QuickCapture, it was used almost exclusively in this thesis. The Image 1.14 program is straightforward to use, but the details provided here will

permit a better understanding of the capabilities and limitations of the program, and will also assist future work in OTR beam profiling.

Like other Macintosh programs, the Image 1.14 program is divided into menus, which are further divided into individual functions. A list of tools provide further options for the user. Procedures will be explained with reference to particular menus, functions or tools.

The first and simplest task which must be mastered is how to capture an image, also known as "grabbing" an image. For the purposes of simply looking at something on a screen, any image will do. However, for the purposes of beam profiling and analyzing data, certain steps must be taken to ensure that the three dimensional beam profile gives useful information. Viewed up close, TV pictures often consist of alternating horizontal lines. One line carries information and varies in color (or intensity on a black and white picture). The other line carries no information, and is either completely black or white. On most TV pictures, this "no-information" line is black, and the Image 1.14 program is initially set up to have black lines for the lines which carry no information.

Through experimentation, it was found that the best procedure for capturing an image was to first establish a good background for the image. By filling the background

with the color black, consistent results were realized. The user chooses the Fill command from the Edit menu to create a uniform black background. Once a completely black picture is on the computer screen, the user chooses the Start Digitizing command under the Functions menu, and captures the image with the Stop Digitizing command. The user must then use the Invert command under the Edit menu to get a three dimensional profile which appears as shown in Figure 9. By using the Invert command, the background is seen as white with an intensity value of zero, and video is seen as gray or black with intensity values between one and 255. If the image is not inverted, the three dimensional plot produced appears to go inward, as shown in Figure 10, rather than outward as in Figure 9.

For the purposes of beam profiling, several useful analytical functions are contained in Image 1.14. As shown in Figure A3 in Appendix A, the intensity profile of an OTR pattern contains much useful information. Image 1.14 has the capability to generate one dimensional intensity scans similar to Figure A3. The Density Profile tool gives an intensity profile versus position for any line drawn on the screen. The width of the line can be 1, 2, 3, 4, 6 or 8 pixels wide, where averaging is performed when the width is greater than one. The vertical scaling can be selected by the user, or automatically scaled by the program. Figure 11

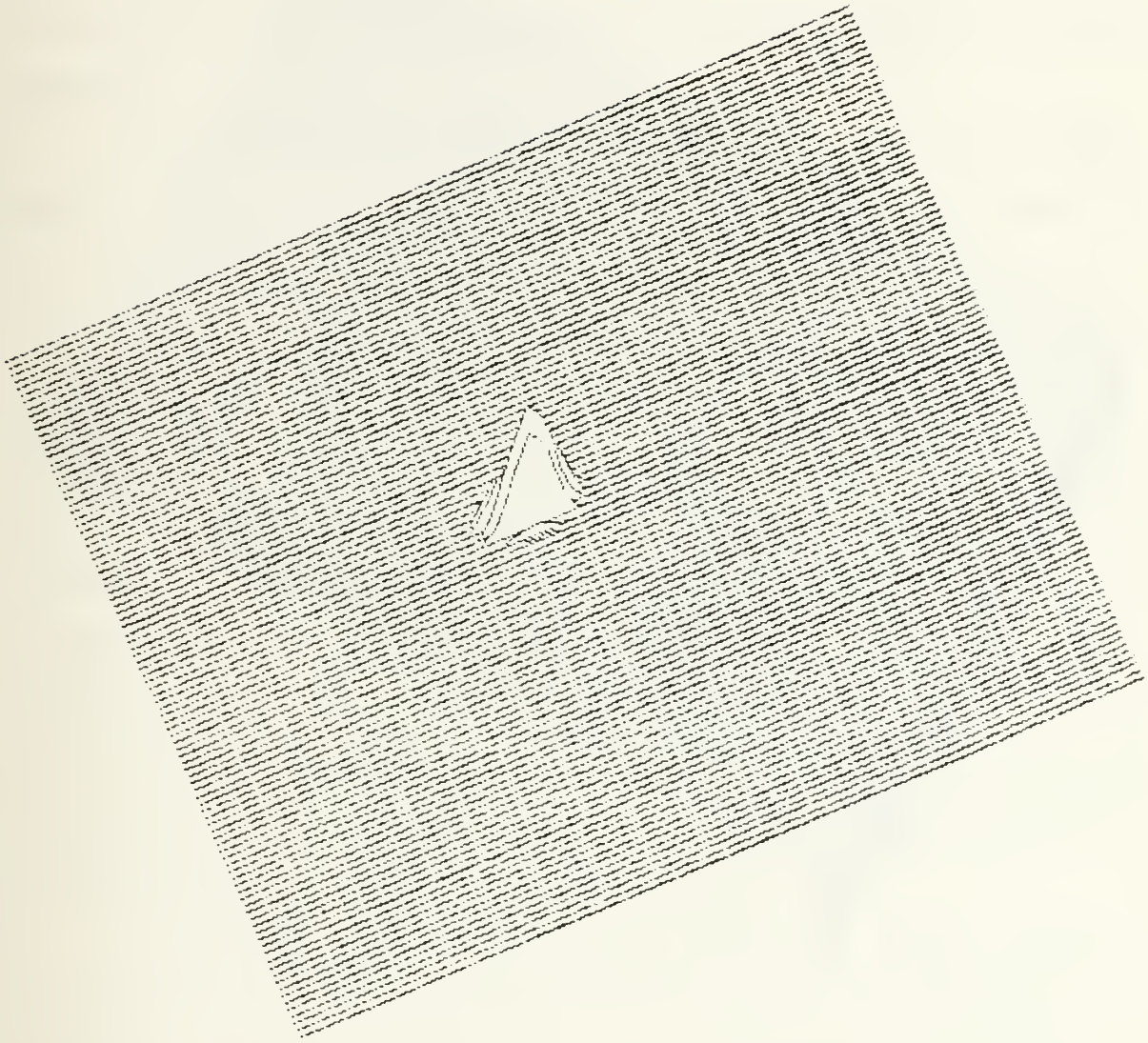

Figure 9: Three-dimensional plot of laser beam spot. This image was captured on a black background and then inverted. (Vidicon, 100 by 100 pixels)

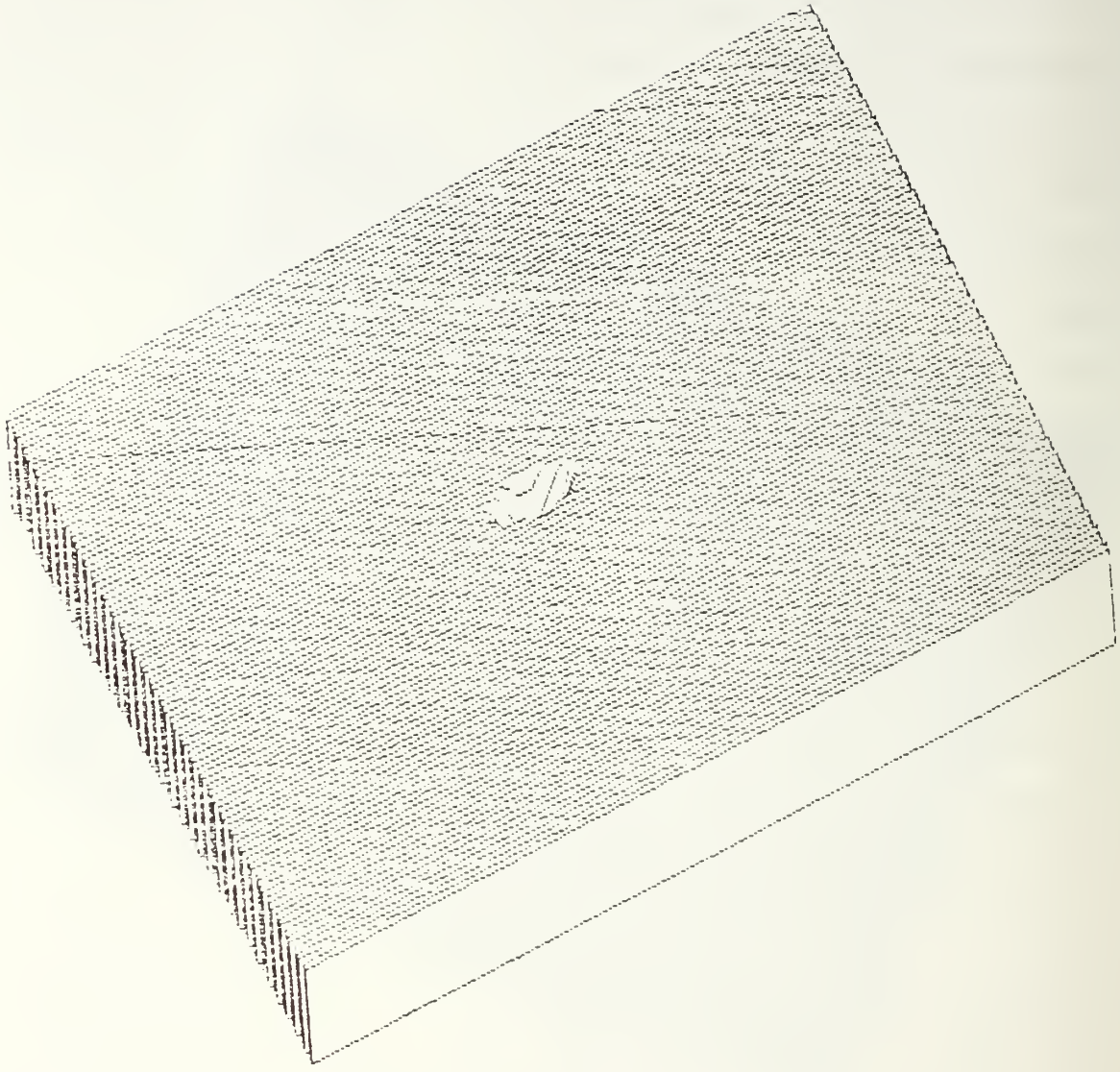

Figure 10: Non-inverted three-dimensional plot of laser beam spot. Compare with Figure 9. This image was taken on a black background also, but was not inverted. (Vidicon, 100 by 100 pixels)

shows a density profile plot with three different pixel widths where the user has selected the scaling of 0 to 255. The Density Profile tool is an used to look at the intensity of individual horizontal line scans. Applied to OTR, this function gives a one dimensional intensity scan of an OTR pattern.

Another function available in Image 1.14 for beam profiling is the Column Average Plot. This function is similar to the Density Profile tool just described, but the user selects a rectangular area of interest instead of a single line. Recall that the Density Profile tool produces an intensity scan for a line with width between one and eight. The Column Average Plot function can produce an intensity scan for a line of any desired width. Figure 12 shows an example of a Column Average Plot. The horizontal width of the plot corresponds to the horizontal width of the user-selected rectangle. The vertical direction of the plot represents the average intensity of the pixels in the corresponding vertical column in the selection.

In addition to intensity scan functions, Image 1.14 also has an Integrated Density function which calculates the density within a particular area of an image. The user selects an area of interest, and the Integrated Density function will give a number for that area according to the following formula:

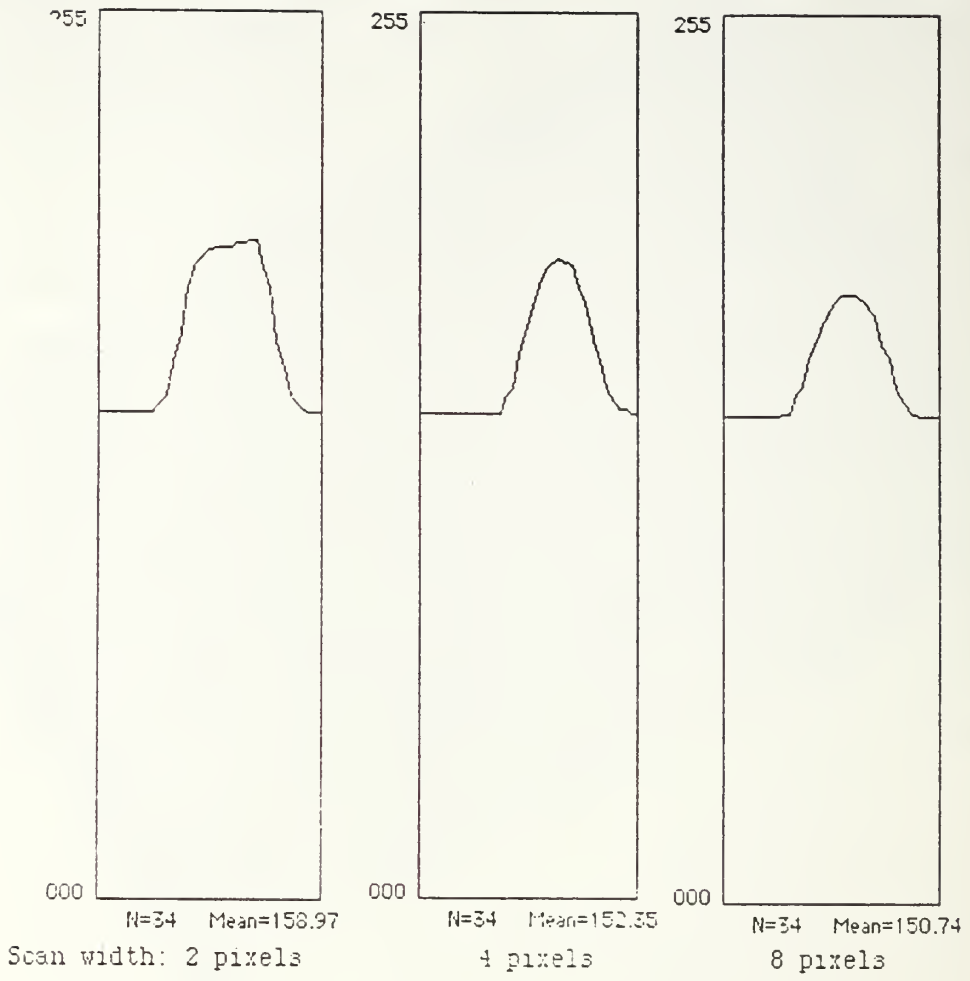

Figure 11: Density profile plot for a laser beam image. This is a one-dimensional line scan of a beam spot. Each line is 35 pixels in length, but vary in width, giving 2, 4, and 8 pixel wide scans. (SITCAM)

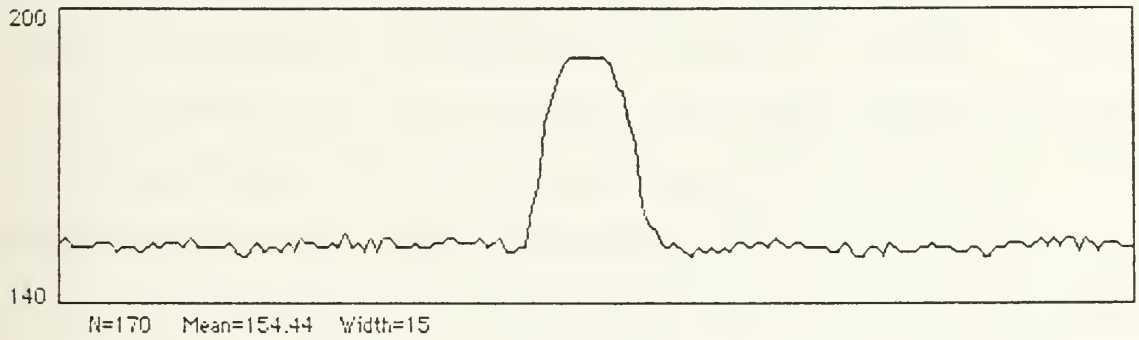

Figure 12: Column Average Plot of a laser beam image. Note the flat top indicates saturation, and there is a large amount of background fluctuation. The area selected was 170 pixels long by 15 pixels wide, camera used was SITCAM.

Integrated Density = N*Mean Density - N*Background Density,

where N is the number of pixels in the selection, and Background Density is the modal density after smoothing. By choosing areas of identical size while keeping the TV camera gain constant, several different images can be compared with the Integrated Density Function. Comparisons of this type appear in the next chapter.

The Functions menu offers an option to Average Frames. The user can select between eight and 100 frames to be averaged before an image is grabbed. Averaging a large number of frames requires a large amount of free memory space on the computer hard disk. The utility of this function is to reduce the effect of background noise. The Average Frames function was found to be useful and will be discussed in the next chapter.

Both the QuickCapture and Image 1.14 programs have a capability to perform arithmetic functions between two images. The user can add or subtract images, and add, subtract, multiply, or divide by a constant to alter the contrast of the image. For example, selecting the subtract option will subtract one image from another, which is useful for finding differences between two images. An application of the subtract option used in this thesis was to subtract a

blank background image from an image that had a laser beam spot on it. The utility of the subtract option will appear in Chapter IV.

The final option under the Analysis menu is the 3D plot, or Three Dimensional Plot. An example of a three dimensional plot has already been shown in Figure 9. It is the most useful analytical function for quick (almost real time) qualitative results. The user can select an area to be plotted, ranging from very small up to the entire picture. Since the three dimensional plot produced by the program is square-shaped, the user should select a square area from the picture in order to maintain proportionality.

In addition to the Analysis menu, there is a Functions menu for manipulating the raw data. It is most likely that these options will remain unused for any actual beam profile measurements. They are essentially filtering functions such as Smooth, Sharpen, Reduce Noise, Dither, and Convolve.

Many other standard Macintosh functions can be found under other menus, such as Cut, Copy, Paste, Rotate, etc. An extensive tools window allows further manipulation of the picture. One noteworthy tool is the Magnifying Glass which can zoom until the screen has a picture seven pixels by nine pixels.

IV. EXPERIMENTAL RESULTS

A. RESULTS

As mentioned previously in Chapter I, this experiment was originally intended to include extensive profiling results from actual OTR measurements. Since the linear accelerator was unavailable to produce an OTR pattern, a laser beam was substituted to provide the source. It should be clearly understood that these results are directly applicable to experimental work on linear accelerators, and especially for OTR experiments. A laser beam has been used to establish a capability to measure optical transition radiation.

1. Lens Scan

Referring back to Figure 1, it can be seen that the intensity of OTR patterns is a strong function of the angle of observation (measured from the angle of specular reflection). In Appendix A, equation 1 also shows the dependence of the intensity on the same angle. Similarly, in this experiment the intensity of the OTR pattern seen by the TV camera is a function of pixel position on the face of the TV camera. Thus, a relationship exists between pixel position and the angular measurement from the optical axis, i.e., the angle between individual pixel position and the optical centerline defined by a specular reflection from the

OTR mirror. The correlation between the pixel position and angular measurement can be seen in Figure 13.

Since the TV camera measures individual pixel position but the OTR intensity is a function of an angular measurement, there must be a method to correlate the measured parameter (pixel position) with the desired parameter (angular position). This method shall be called a lens scan. The equipment setup for a lens scan is shown in Figure 14, and is a minor modification of the original experimental setup shown in Figure 2.

The procedure for a lens scan is straightforward. With the TV camera on and the laser beam centered on the focusing lens, the rotating mirror is rotated through 360^{o}. The controller for the rotating mirror gives a digital readout of position, and this can be equated to 2π radians. It was found that one radian corresponded to 43,340 units on the controller, and so one milliradian equaled approximately 43.34 units. This angular measurement was then converted to pixels by scanning across the focusing lens between two points. It was further found that 8.31 units on the rotary stage controller corresponded to 1 pixel on the Macintosh II PC. (The output of the TV camera is viewed directly on the computer.) Thus, one pixel on the Macintosh II PC equals 600 microradians for this particular setup.

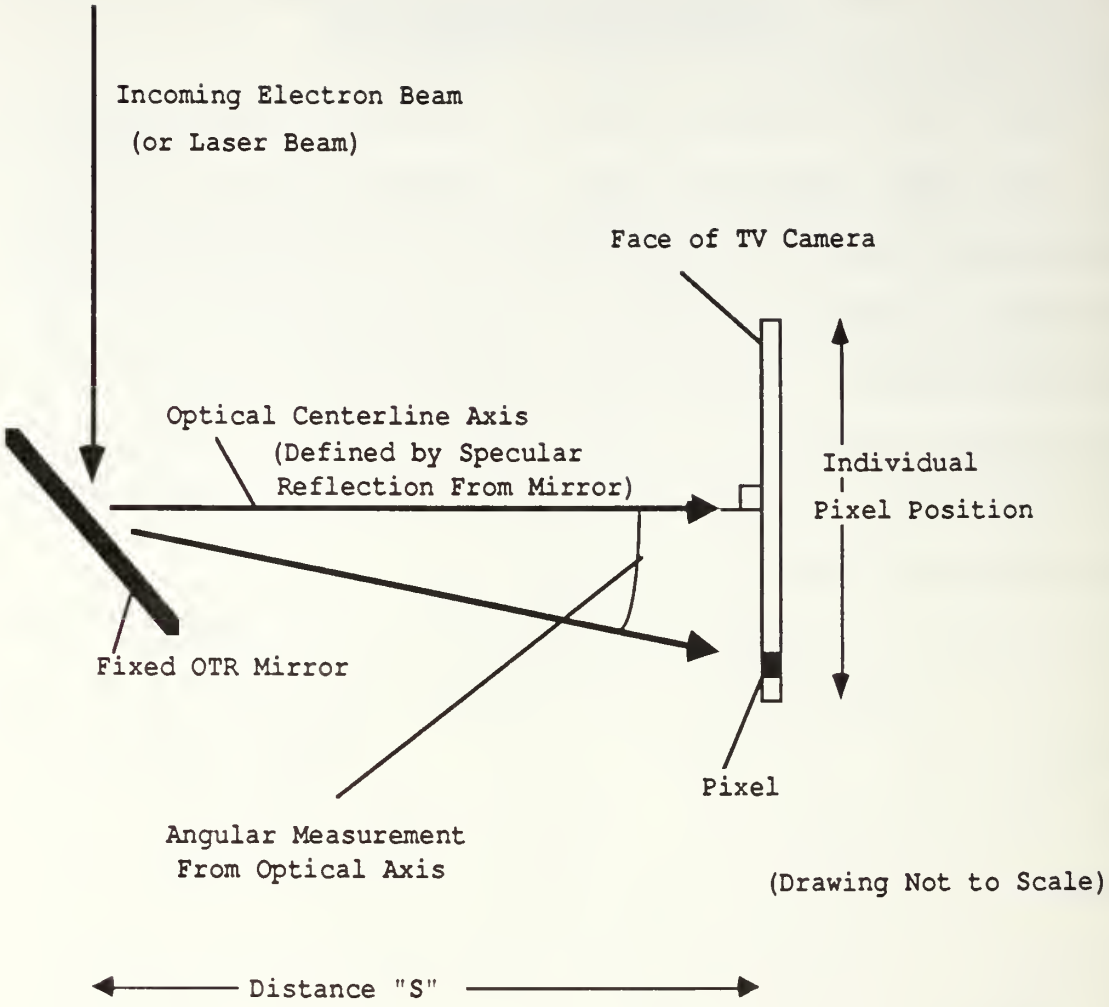

Figure 13: Intensity of OTR pattern as a function of angular measurement and pixel position. Intensity of the OTR pattern is sensed at the TV camera by individual pixel position, which must be correlated to an angular measurement from the optical centerline.

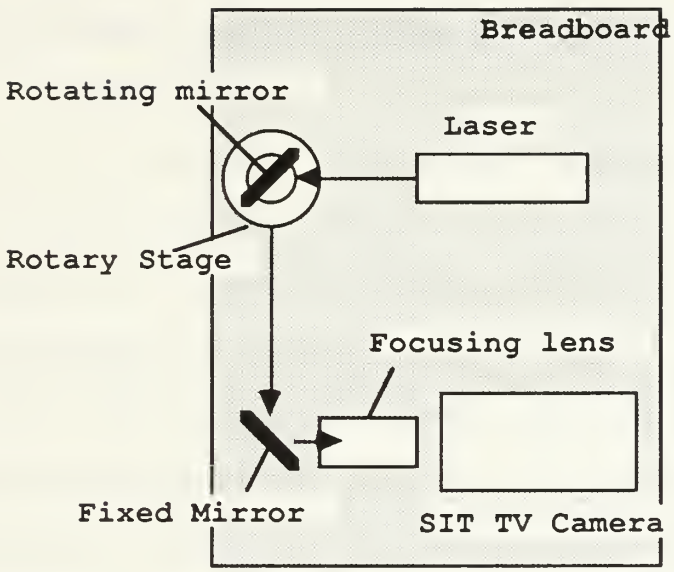

Figure 14: Equipment setup for a lens scan. Note this is only a slight modification of the experimental setup shown in Figure 2.

In order for the lens scan to properly correlate pixel position and angular measurements, one critical distance must be realized. The distance from the center of the rotating mirror (where the laser beam reflects off it) to the focusing lens (distance "S" on Figure 13) should be as close as possible to the distance from the OTR mirror to the focusing lens. By placing the rotating mirror the same distance from the focusing lens as the OTR mirror, the angle of the lens scan will equal the angle from an OTR pattern.

2. TV Camera Response

The response of two types of TV cameras was investigated with the IMAGE software: a common Vidicon for everyday applications, and a silicon-intensified target TV camera (SITCAM) designed for low light level use. The Vidicon carried information on every horizontal line of pixels, whereas the SITCAM carried information only on every other line. Both of these cameras have manual gain control so that camera gain could be kept constant. Constant gain of the TV camera is an important feature when comparing one image to another. A camera with automatic gain will respond differently for images with different light levels.

The intensity of the light entering the TV camera can be changed by inserting neutral density filters in the path of the laser beam. Neutral density filters are specified in terms of their optical density, D. Optical density is a

measure of the filter, such that the higher the optical density a filter has, the greater the attenuation of the light going through it. Optical density, D, can be defined as the base 10 logarithm of the inverse of the transmittance, T:

$$D = \log_{10} (1/T),$$

where T is the transmittance of light through the filter. An optical density of 1 will transmit 0.1 of the light incident upon it. If optical density is 2, then transmission is 0.01, etc. When stacked in series, optical densities are additive, such that $D_{total} = D_1 + D_2 + D_3$. [Ref 15]

In this experiment, it was found that if the optical density of the filters inserted in front of the laser beam were too great, the beam spot was not visible. Conversely, an optical density which was too low meant that the laser light saturated the TV camera, producing a flat-topped beam profile, shown in Figure 15. The SITCAM seemed much more susceptible to saturation. The user must use the proper amount of filtering to prevent saturation, which is determined through experimentation.

3. Background Noise

In addition to the saturation problem just mentioned, the TV cameras also exhibited a large amount of background noise, i.e., the intensity variation of individual pixels.

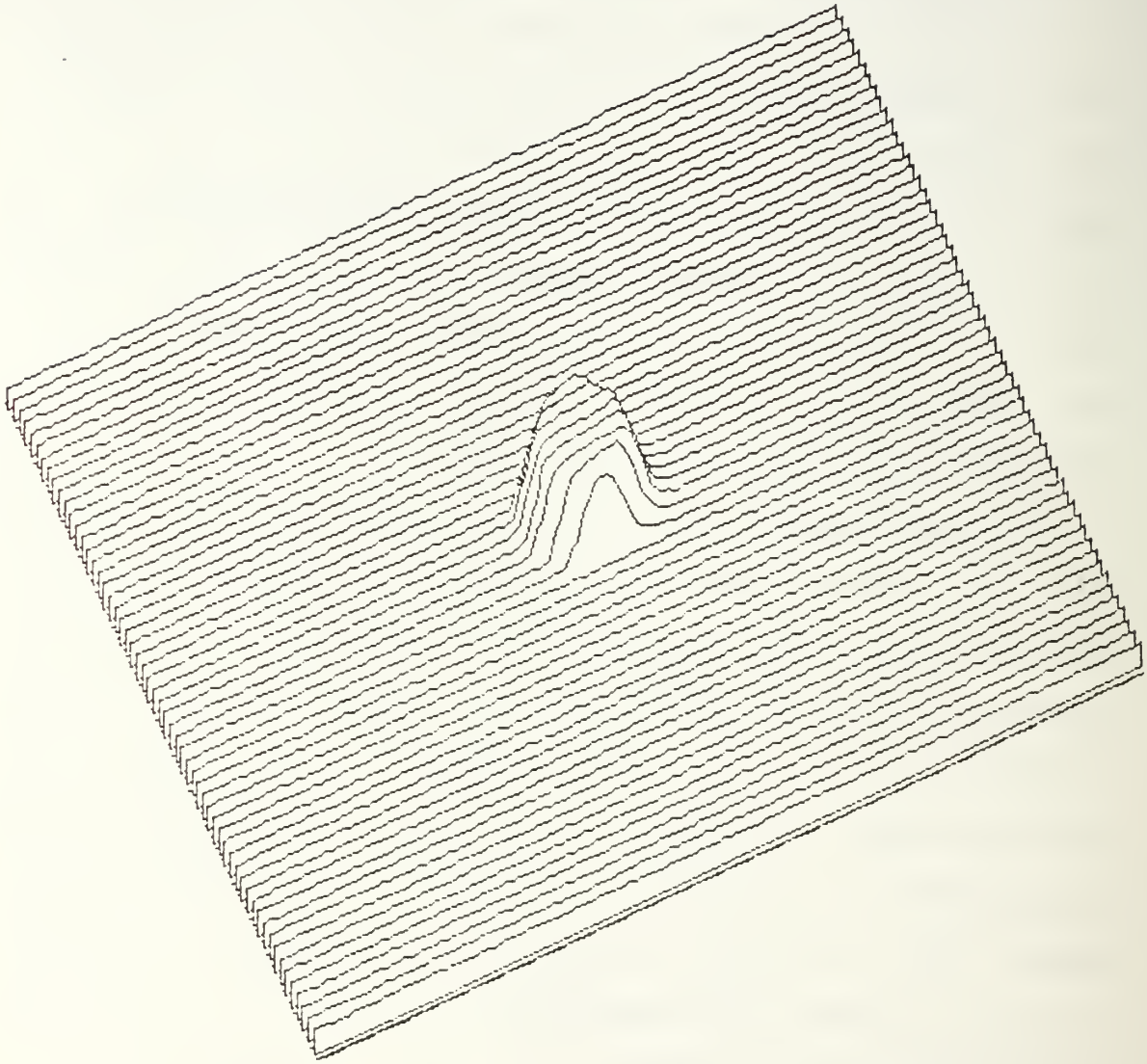

Figure 15: Flat-topped beam profile. Flat-topping is caused by saturation of the TV camera (SITCAM).

Pixel intensity of a blank background varied a great deal, sometimes as much as 25 or even 30 units on a 256 unit intensity scale. The level of variation in the background is of concern so that some level of confidence can be placed in intensity measurements for an individual pixel. Therefore, by determining the variation of intensity in the background, one can also determine what is a significant intensity variation and what must be considered simply systematic error or noise.

As can be seen in the column average plot of Figure 16, the background level varies considerably. The width of the column average plot in Figure 16 is 25 pixels, which means that 25 pixel intensity values from the image were averaged to calculate one intensity value for the plot. Since the intensity of the background as shown on the plot is not constant, this indicates the background intensity of the image is varying considerably.

Upon closer examination of the experimental setup, it was found that the digitizer, computer with frame grabber, and auxiliary TV monitor were all on separate power sources. This mismatch of power sources introduced interference between the 60 Hertz inputs to the digitizer, computer, and monitor. Sufficient interference was introduced to cause alternating light and dark horizontal bands to move up the TV monitor screen and also the PC screen. The interference

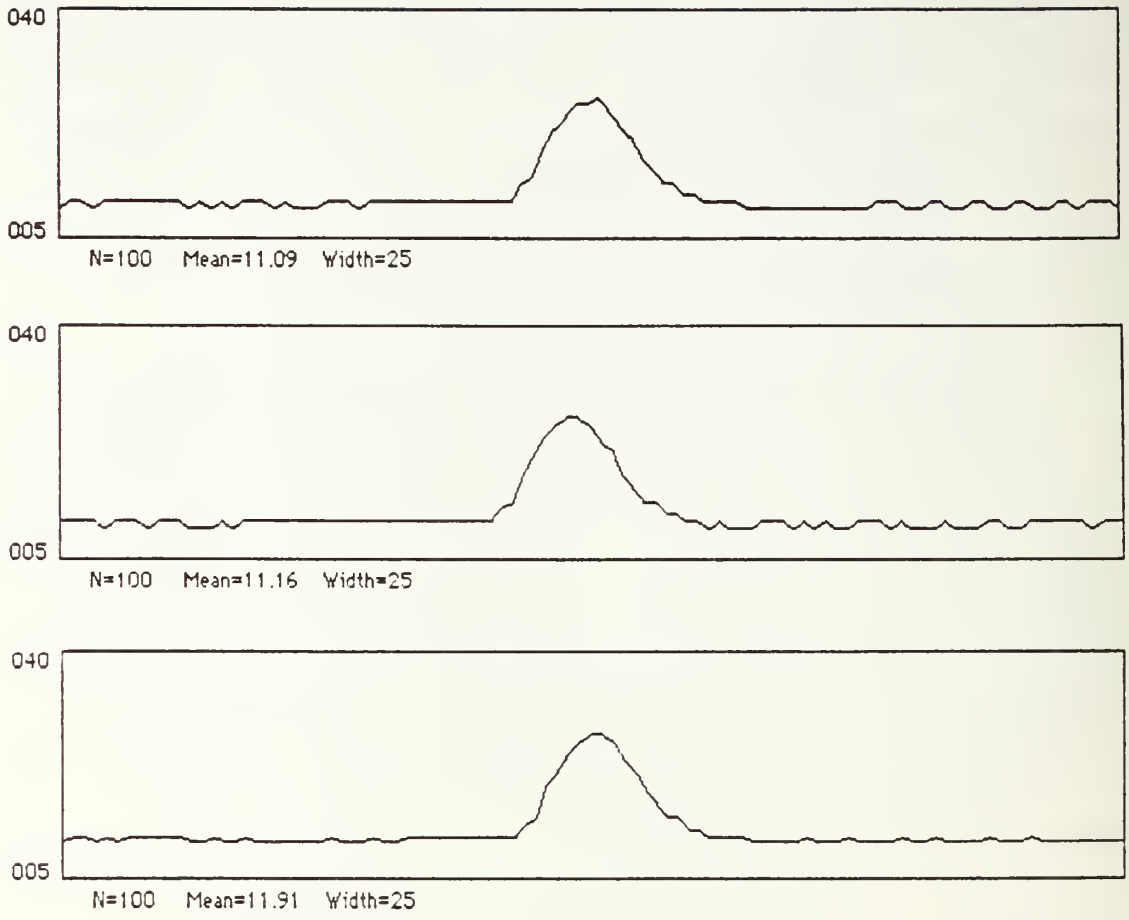

Figure 16: Column Average plot of three images taken under the same camera conditions. Note the high level of background variation, due to electronic components on separate power sources. The area selected is 100 pixels long by 25 pixels wide, camera used was Vidicon.

caused large variations in the intensity of individual pixels as seen on the computer screen, and also in the captured images.

The TV monitor derives its vertical synchronization from the camera and camera control unit (CCU). Since the monitor and PC were on separate 60 Hertz power lines, they were not synchronized with the camera and camera control unit. By placing all four pieces of equipment (TV camera, CCU, monitor, and PC) on the same power source, the vertical synchronization was achieved. The horizontal bands moving up the screen were eliminated and individual pixel intensity variations were down to five intensity units. Figure 17 shows the column average plots of three laser spots taken with reduced background noise. These three pictures give remarkably similar results: a steady background, a similar mean value, and similar beam profile. Thus, a means for establishing a low background noise level has been established.

4. Qualitative Results

Up to this point, the discussion has been limited to methods of obtaining digital images, calibrating results to match experimental setup, and reducing gross background fluctuations. Now, the discussion will focus on methods of comparing measurements between two or more images. The measurements will be both qualitative and quantitative.

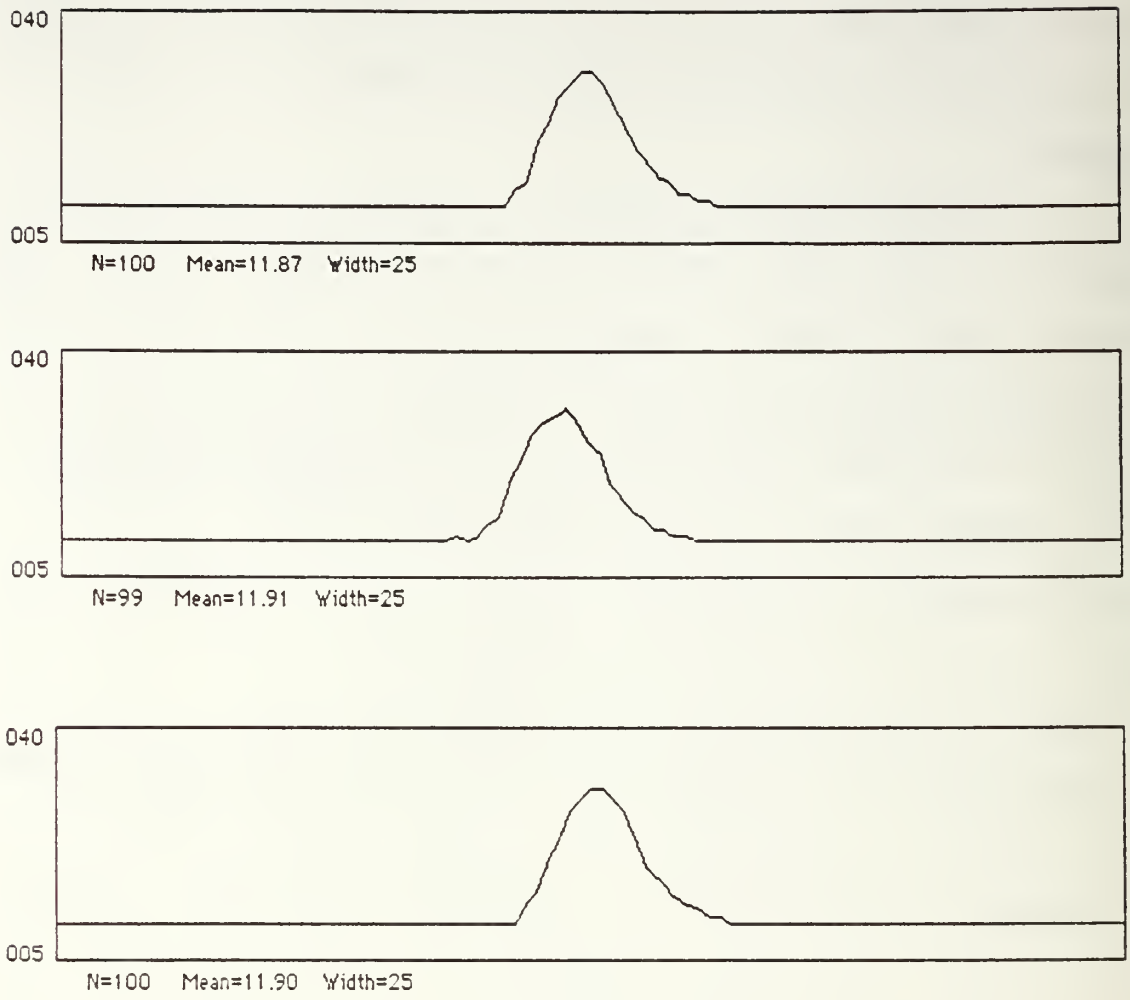

Figure 17: Column Average plot of three images taken under reduced background level conditions. High background noise level has been reduced by drawing electrical power from same source for computer, digitizer, camera control unit, and auxiliary TV monitor. Compare with Figure 16. The area selected is 100 pixels long by 25 pixels wide (same as Figure 16). (Vidicon)

Optical transition radiation measurements require an extremely fine capability to measure intensity, a measurement of the order of less than one percent error. Since OTR patterns were not available for viewing and measuring intensity, a laser beam was used to provide the image. By comparing several images of the same source, one can obtain an idea of the capabilities of the experimental setup.

In this section, qualitative results will be discussed. The single qualitative measurement used was the three-dimensional plot.

Several images of a laser beam were taken successively (under the same camera conditions) in order to determine to what degree the image stays constant. Three-dimensional plots from three different images are shown in Figures 18, 19, and 20. Note that although individual pixel intensities are varying within the beamspot giving slightly different intensity profiles, the overall profile appears to remain constant. This suggests that a qualitative result such as a three-dimensional beam profile will remain constant without significant deviation. For an OTR experiment, one could easily verify the reproduceability of the OTR pattern by using this same idea.

Another effect which was investigated was that of altering the orientation of the neutral density filters. Images of a laser beam were taken with the filters at three

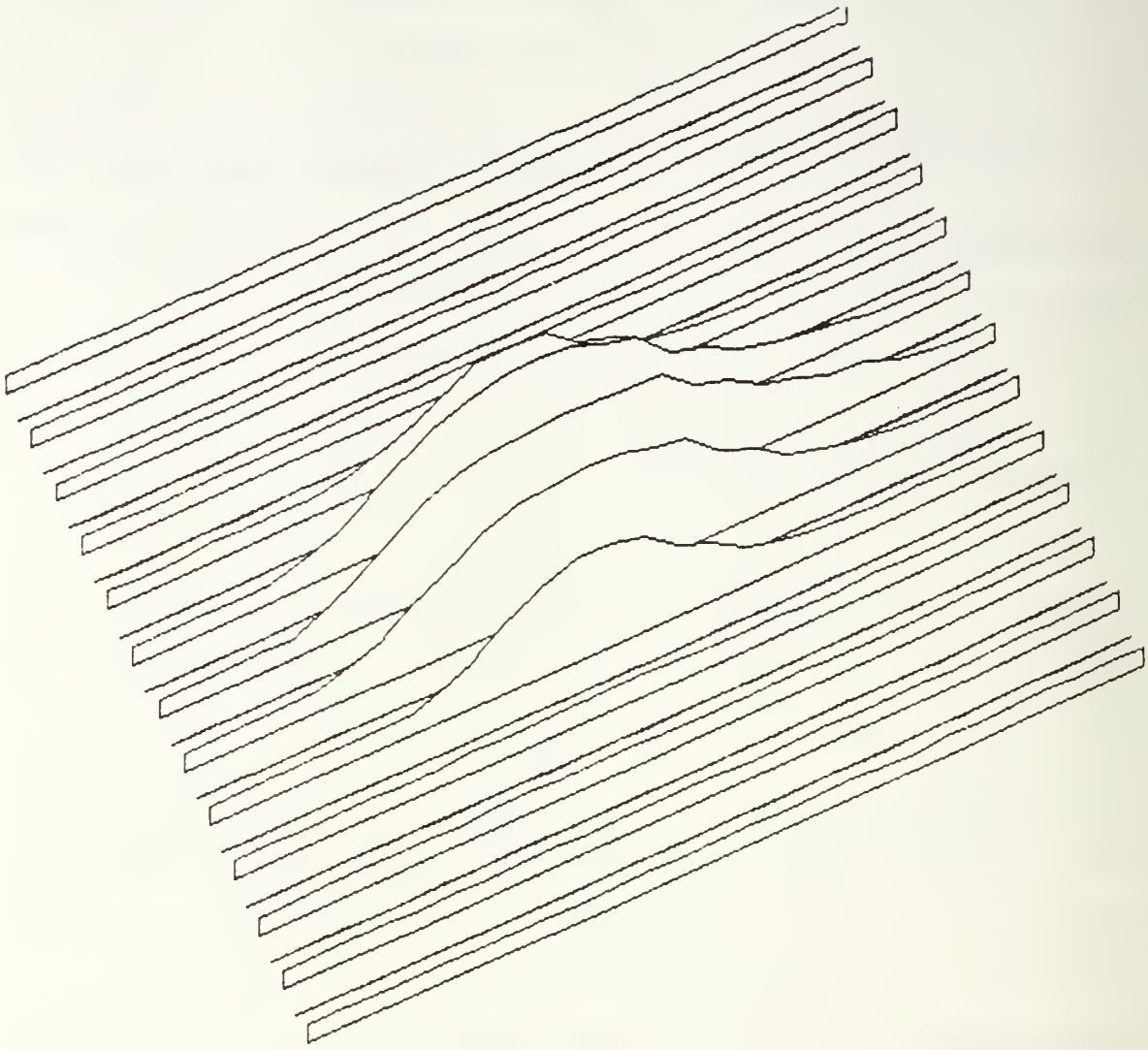

Figure 18: Beam profile of laser spot image. Compare with following two figures which were taken successively under the same camera conditions. Note that the beam profile remains essentially constant between the three figures. The area chosen was 25 by 25 square pixels (SITCAM).

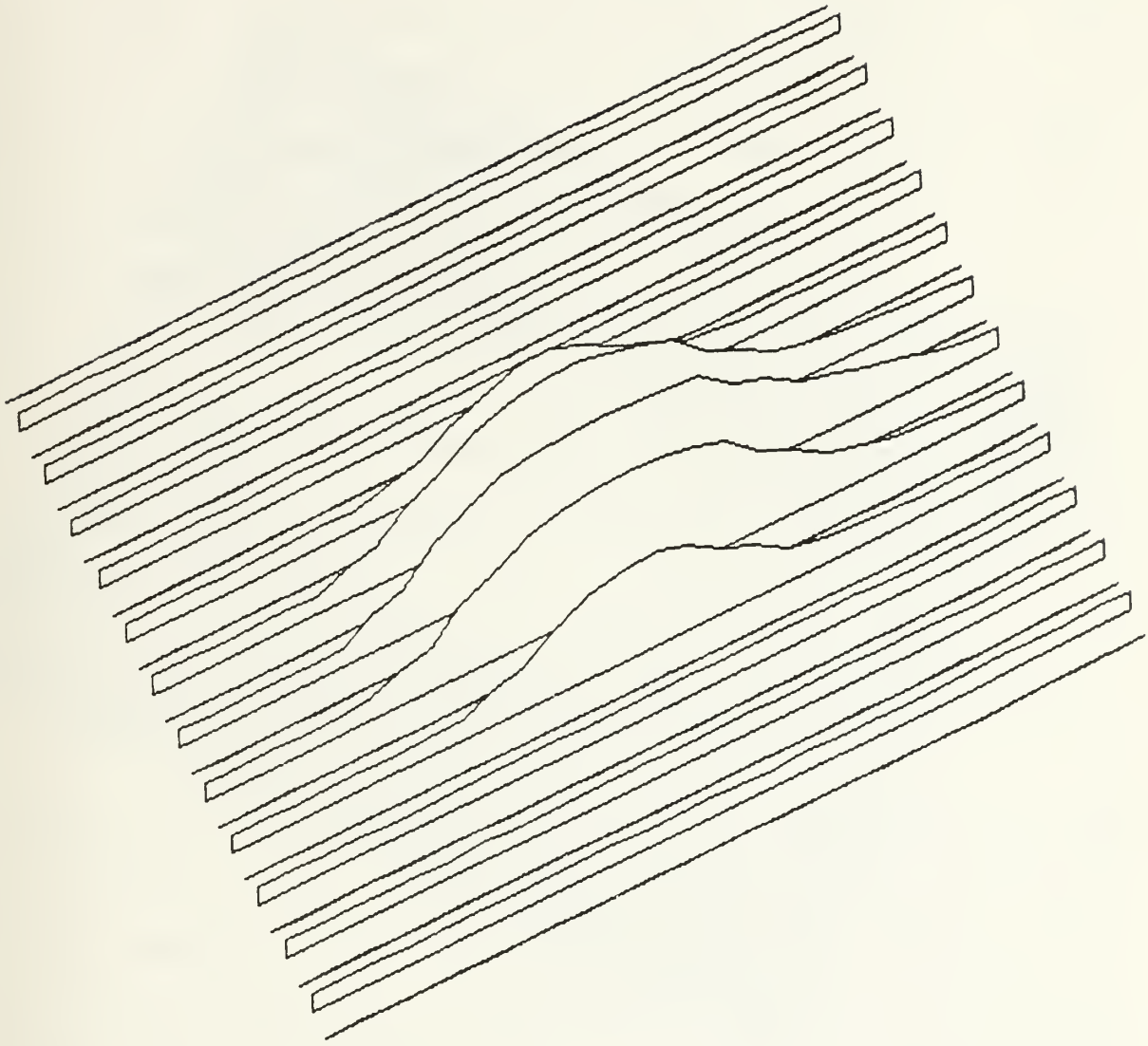

Figure 19: Beam profile of laser spot image taken under same conditions as Figures 18 and 20. Beam profile appears to stay constant. Same area chosen as Figure 18 (SITCAM).

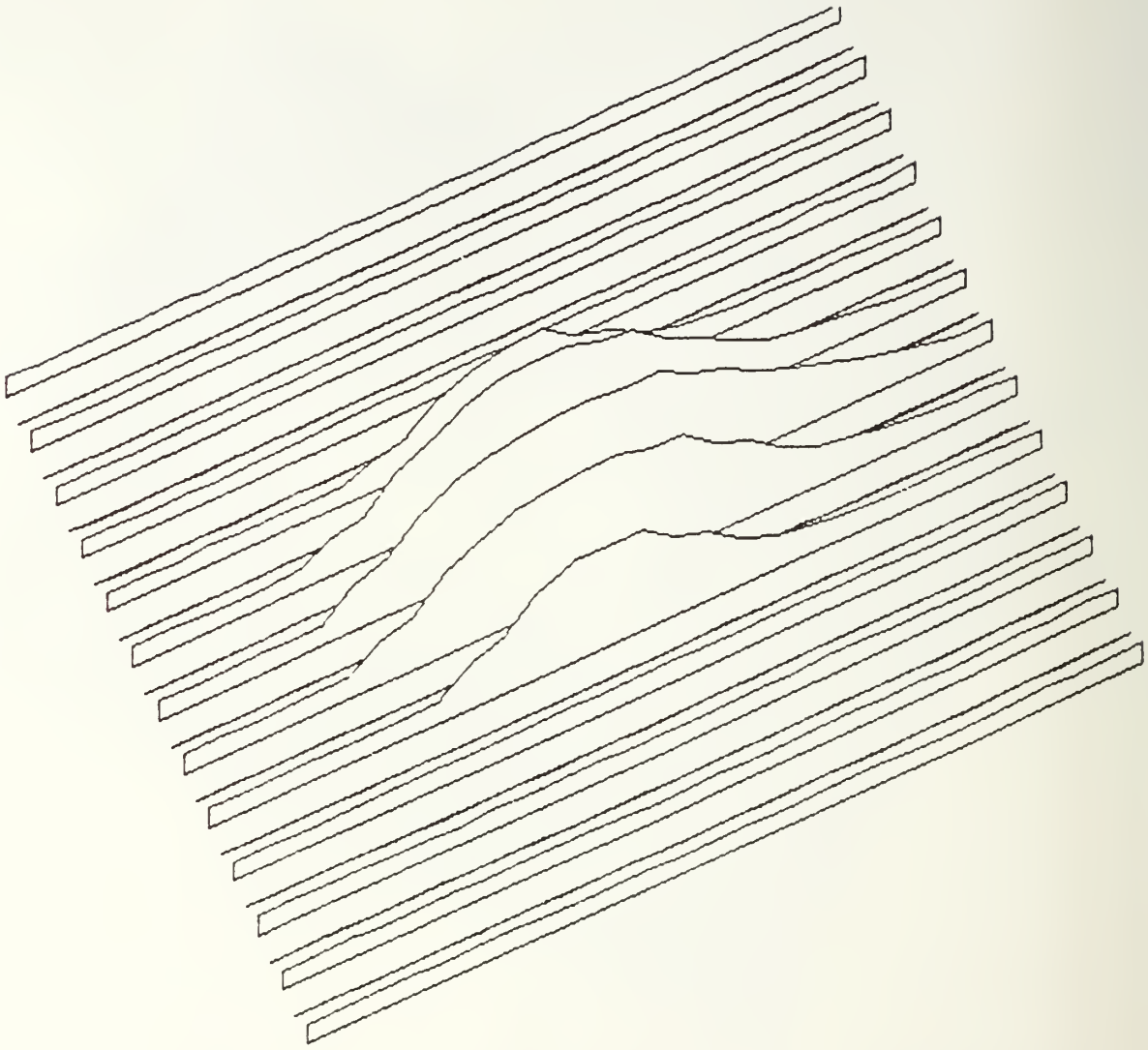

Figure 20: Beam profile of laser spot image taken under the same conditions as Figures 18 and 19. Note only slight changes between the three images. Same area chosen as Figures 18 and 19 (SITCAM).

different positions: normal to the beam, just offset from normal, and offset at approximately 45°. The effect is shown in Figures 21, 22, and 23. The three-dimensional plot for the normal and off-normal case are nearly identical. The plot for the 45° case is greatly diminished in height. It can be seen that the three-dimensional plot is a useful tool to produce qualitative results for beam profiling.

5. Quantitative Results

In addition to the qualitative result above, Image 1.14 provides a capability to produce quantitative results. The quantitative measurement method chosen was the integrated density function. Recall from Chapter III how integrated density is calculated:

Integrated Density = N*Mean Density - N*Background Density,

where N is the number of pixels in the selection and Background Density is the modal density after smoothing. (Modal density is the most frequently occurring density level within the selection.) Because the intensity of the beam image above the background is of primary interest, the integrated density function was the chosen method of measurement. It can quickly produce a number which represents the intensity of a selected area. In the figures shown in this section, several images were taken successively

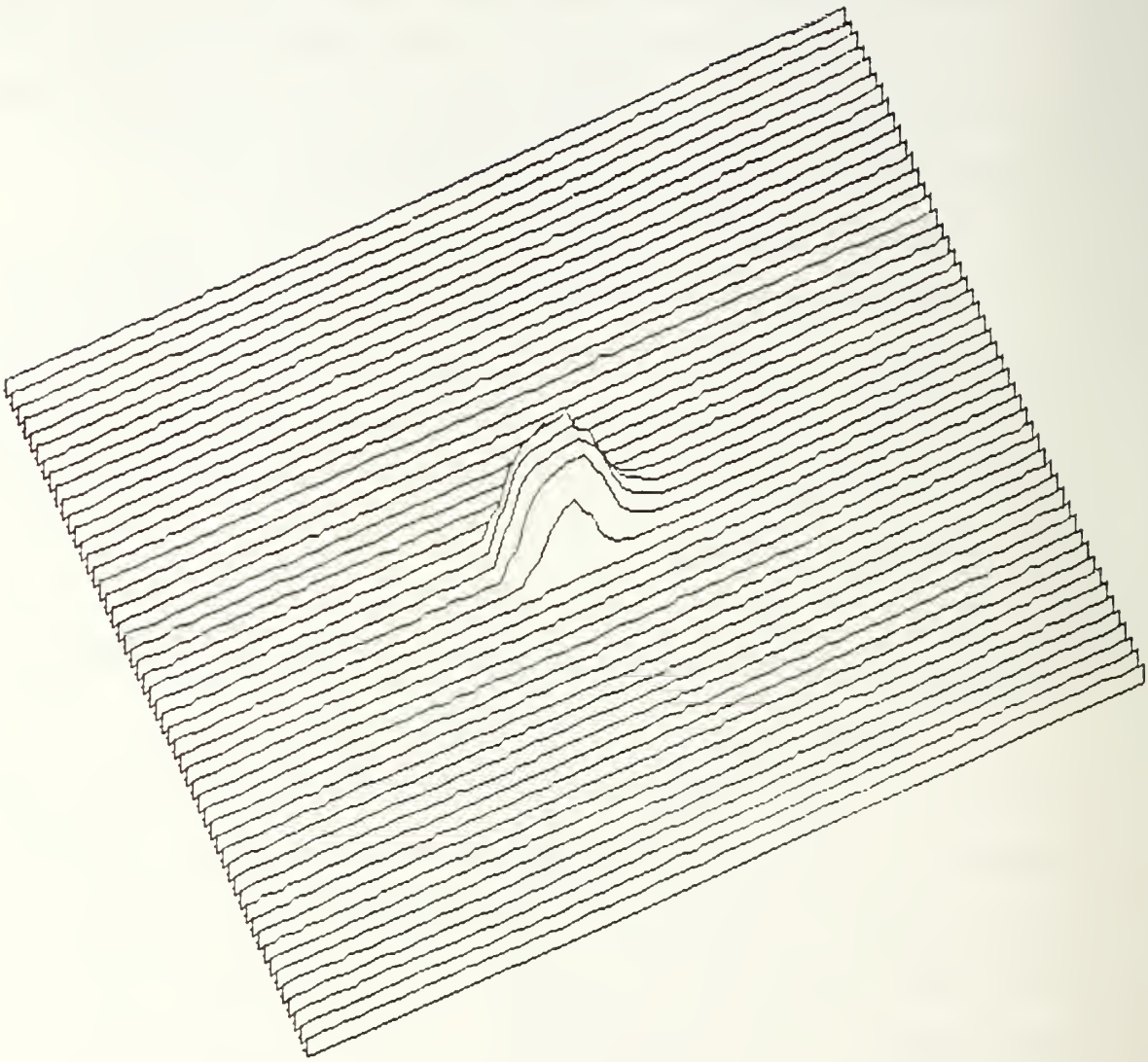

Figure 21: Beam profile of laser beam with neutral density filters oriented perpendicular to the beam path. Compare with the following two figures (SITCAM).

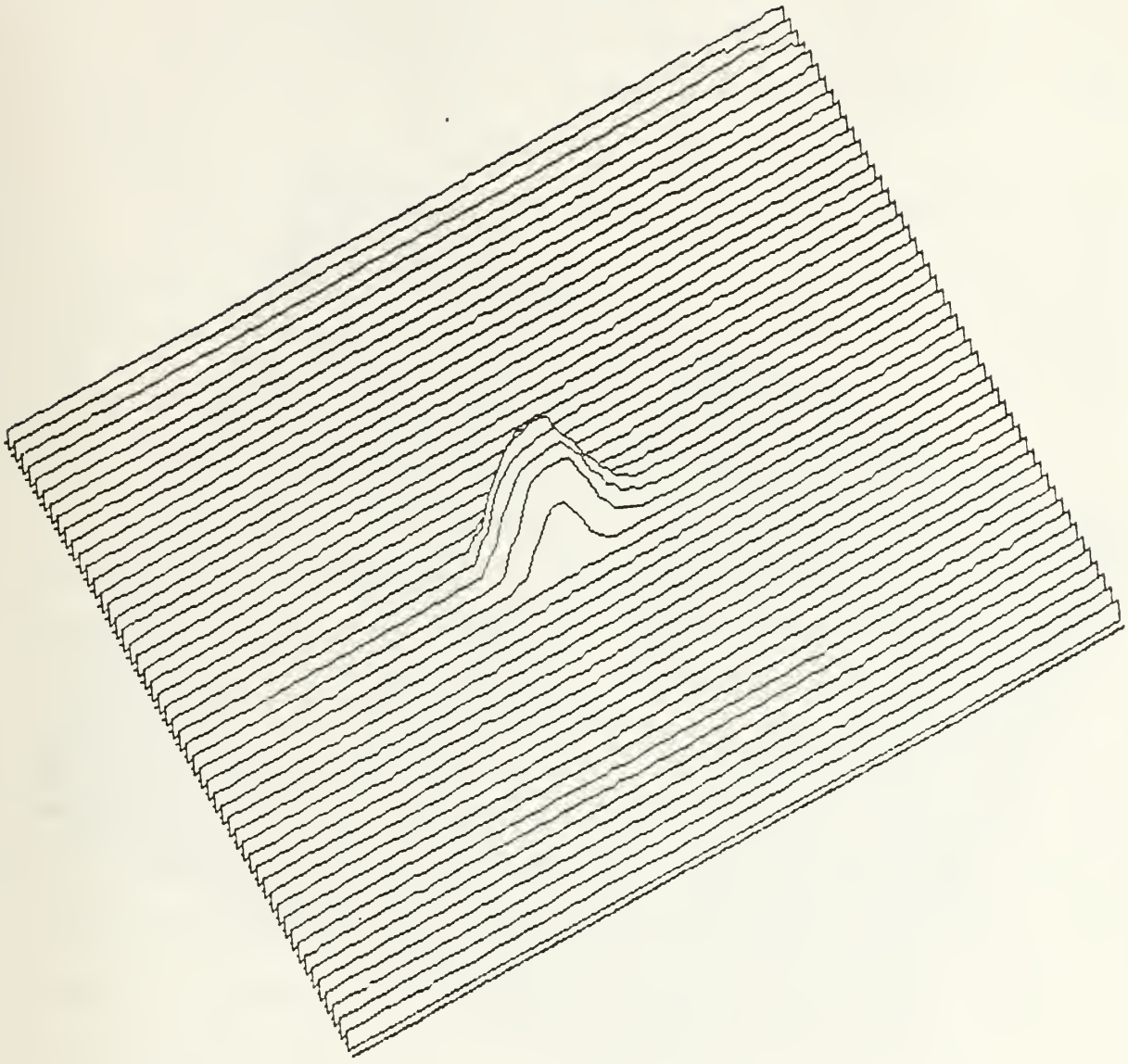

Figure 22: Beam profile of laser beam with neutral density filters slightly offset from perpendicular to laser beam path. Compare with preceding and following figures. Note that this figure appears very similar to Figure 21 (SITCAM).

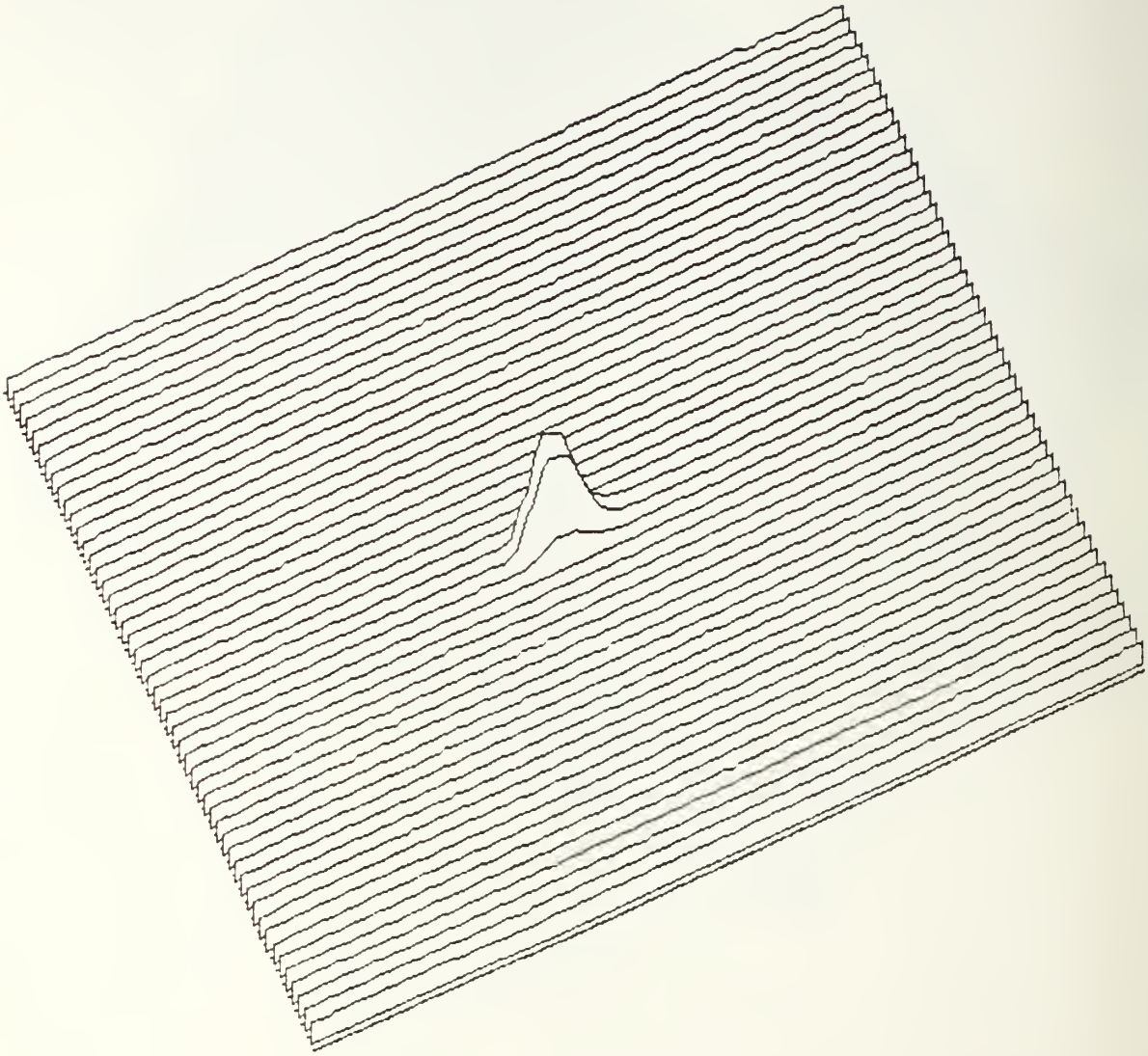

Figure 23: Beam profile of neutral density filters oriented at 45° to laser beam path. Compare with Figure 21 and 22 to notice the large reduction in intensity (SITCAM).

with the camera gain held constant. The integrated density of a constant area was taken for each image, and each integrated density value is normalized with respect to the average of all values for the run.

Figures 24 and 25 illustrate the variation of integrated density for several images taken successively. The SITCAM TV camera was used to capture images of the laser beam, but camera gain was changed between the two runs. A significant variation of about 10% is seen.

As mentioned above in the quantitative results section, the orientation of neutral density filters was examined. Figure 26 shows the results for filters oriented normal, and just off-normal to the laser beam. The 45° offset is not shown. The off-normal average is not referenced to 1.0, but rather is referenced to the average for the normal case. The off-normal case shows a decrease in integrated density. By orienting the filters offset from the normal, a longer path for attenuating the beam is presented, so a decrease in intensity is expected.

The effect of filter position was also examined. As shown in Figure 27, the filters were placed at position 1, directly in front of the laser; and also at position 2, at a great distance from the laser. Figure 28 shows the results of the Integrated Density function for these two cases. The intensity was higher when the filters were directly in front

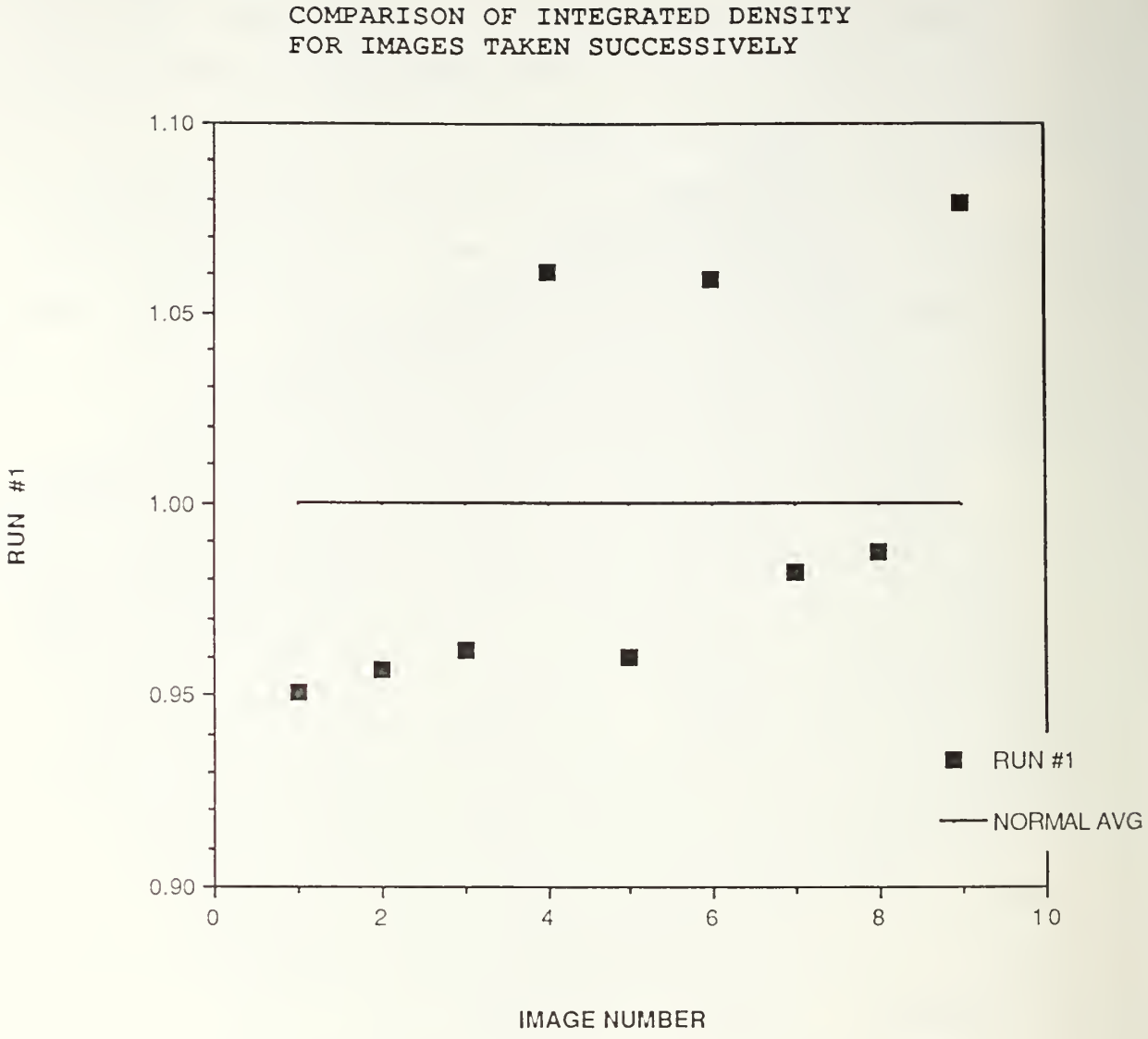

Figure 24: Comparison of integrated density for several laser beam images taken successively under the same camera conditions. Compare with Figure 25. Note large variations in values. Integrated density values have been normalized to the average of all values for this run (SITCAM).

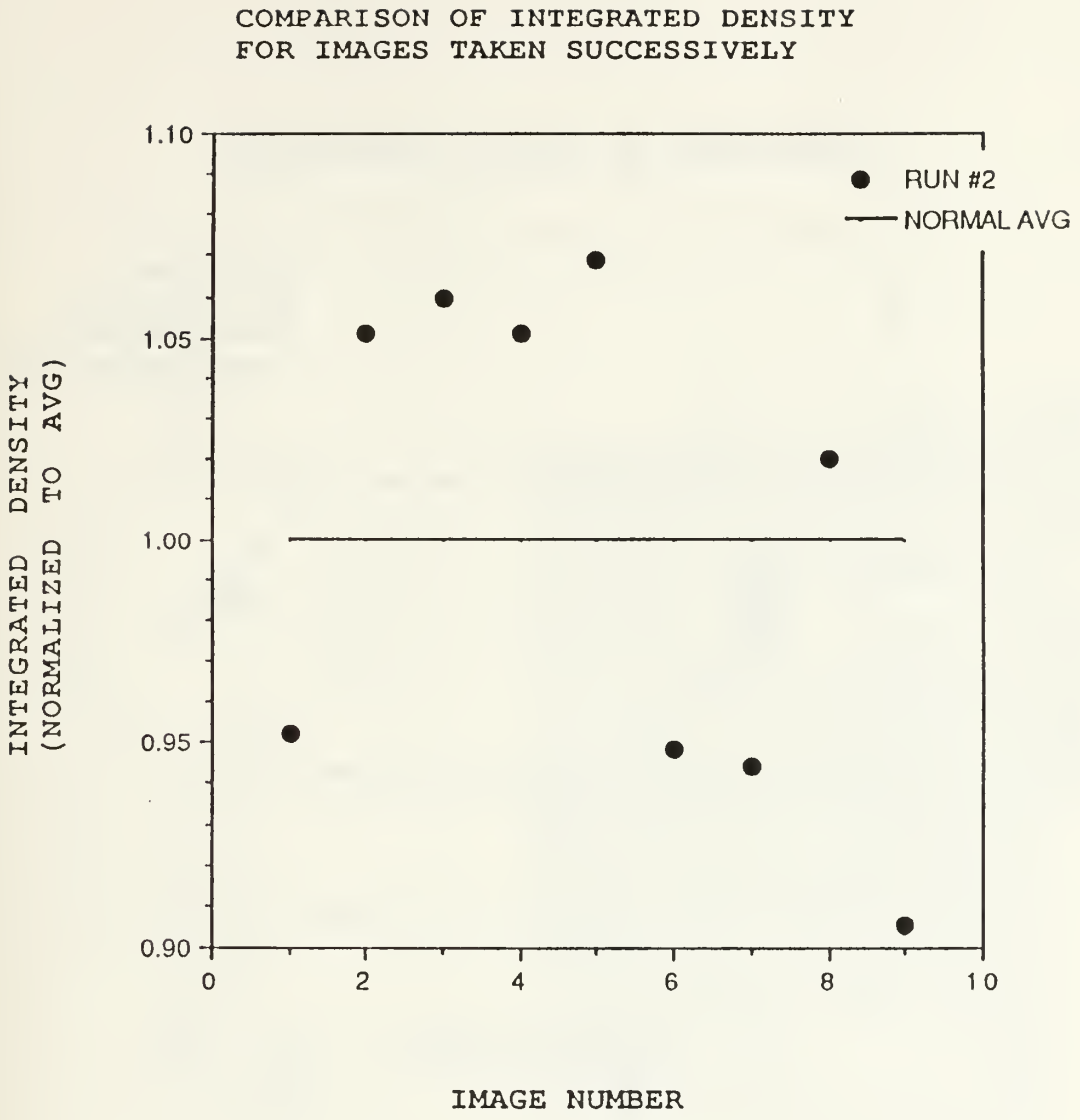

Figure 25: Comparison of integrated density values for several laser beam images taken successively under the same camera conditions. Compare with Figure 24. Large variations are evident. Integrated density values normalized to the average of all values for this run (SITCAM).

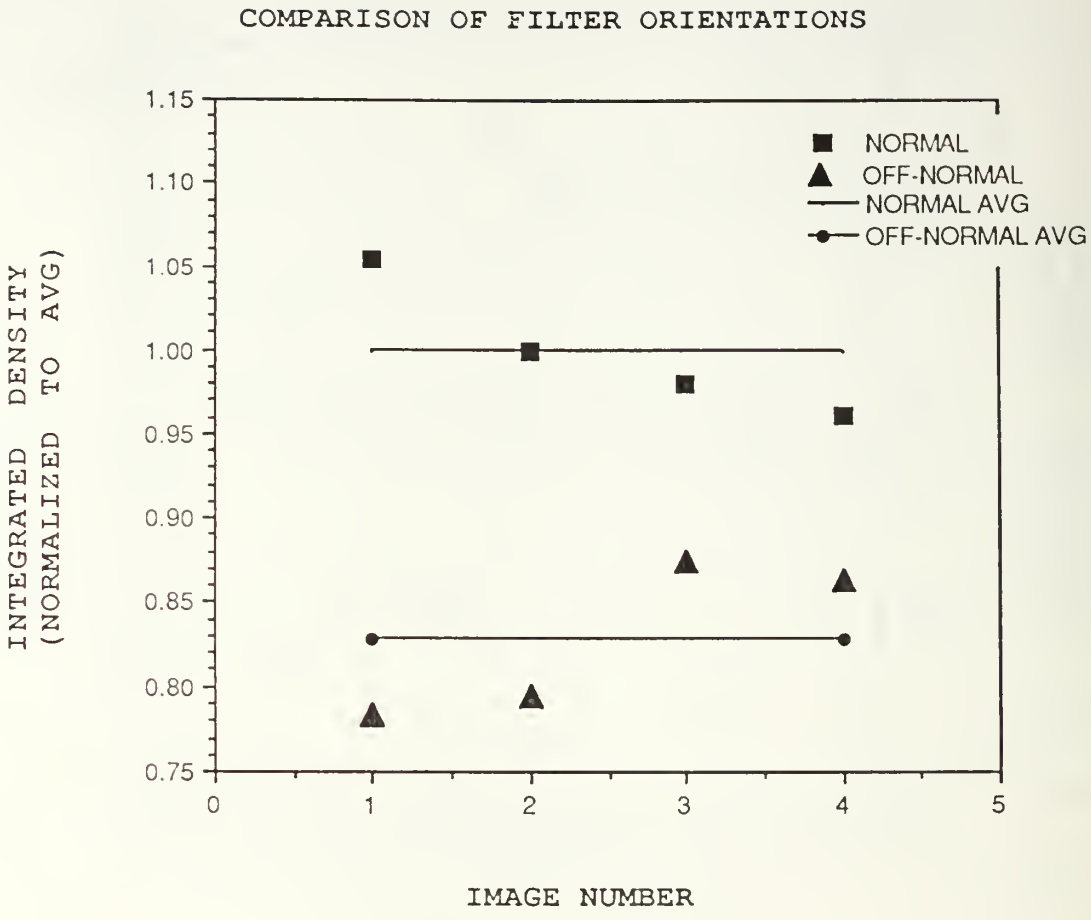

Figure 26: Comparison of normalized integrated density values of successive laser beam images for two orientations of the neutral density filters. The off-normal case shows a decrease in the integrated density. All values normalized to the average for the normal case (SITCAM).

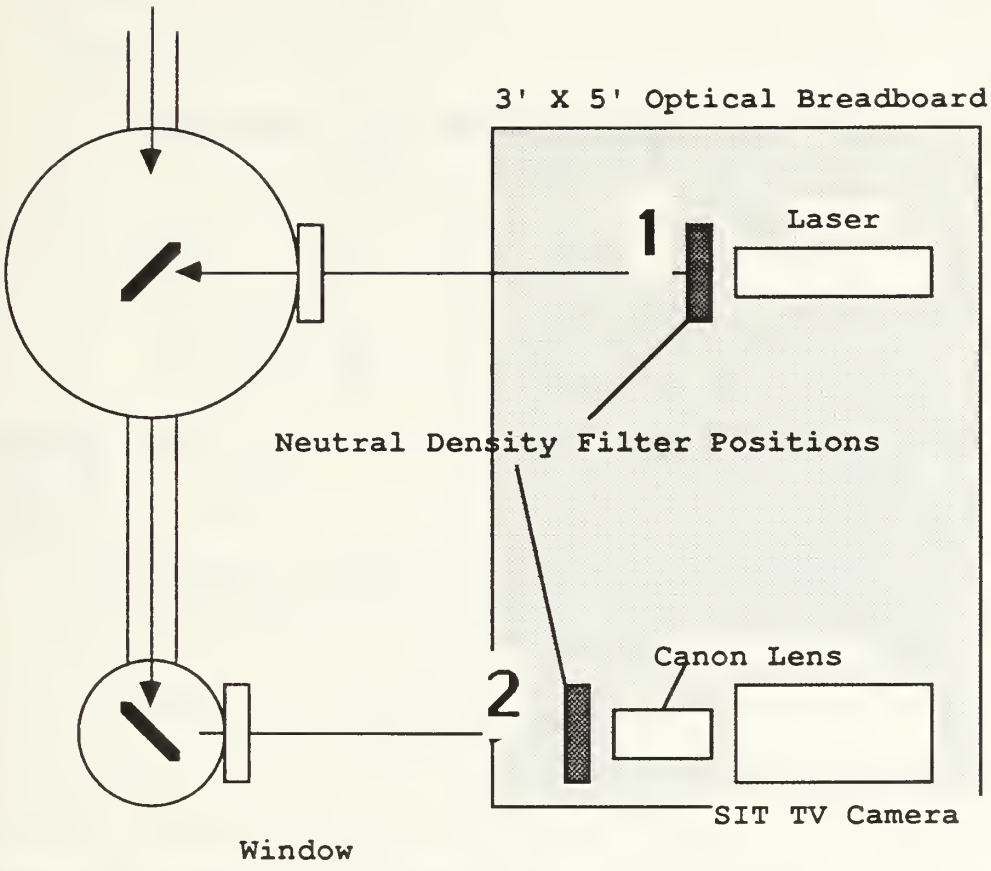

Figure 27: Filter positions 1 and 2. This is the same basic experimental setup as shown before in Figure 2.

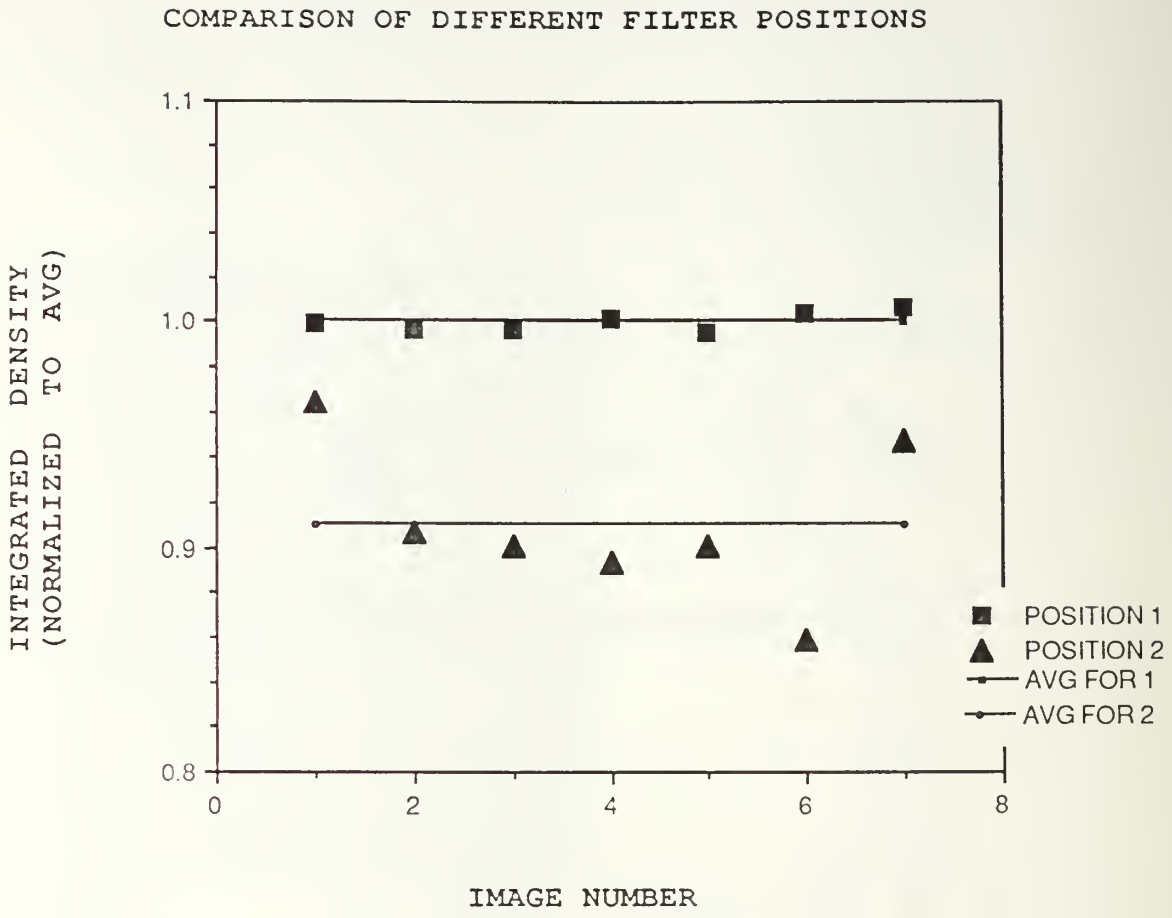

Figure 28: Comparison of normalized integrated density values for different filter positions of laser beam images. Position 1 is directly in front of the laser, position 2 is far away from the laser. Note that the integrated density is higher when filters are in position 1. All values normalized to the average for the position 1 case (SITCAM).

of the laser beam at position 1. Since the filters diverge the laser light, this result was unexpected. A possible explanation may be that the focusing lens causes the divergent light to be focused, giving a more intense picture.

By varying the optical density of the neutral density filters reducing the laser light, another filter effect was seen. As mentioned previously in section 2 of this chapter, a specific increase in the optical density of the filters corresponds to a certain decrease in the intensity of the transmitted light. The optical density of the filters was increased by 0.1, which should result in a 26% decrease in intensity. The results are shown in Figure 29. (All integrated density values are normalized to the average for the optical density 5.8 case.) Increasing the optical density causes the integrated density to decrease, which is expected, but the 26% reduction factor is not seen. The reduction is more of the order of 6%, which indicates that the capability to measure relative intensity between two images must be investigated further. Also, there remains a significant variation in individual values for the integrated density function.

The results shown above in Figures 24, 25, 26, 28, and 29 consistently show a large fluctuation in the value of integrated density between several images taken under the same camera conditions. Investigative efforts toward

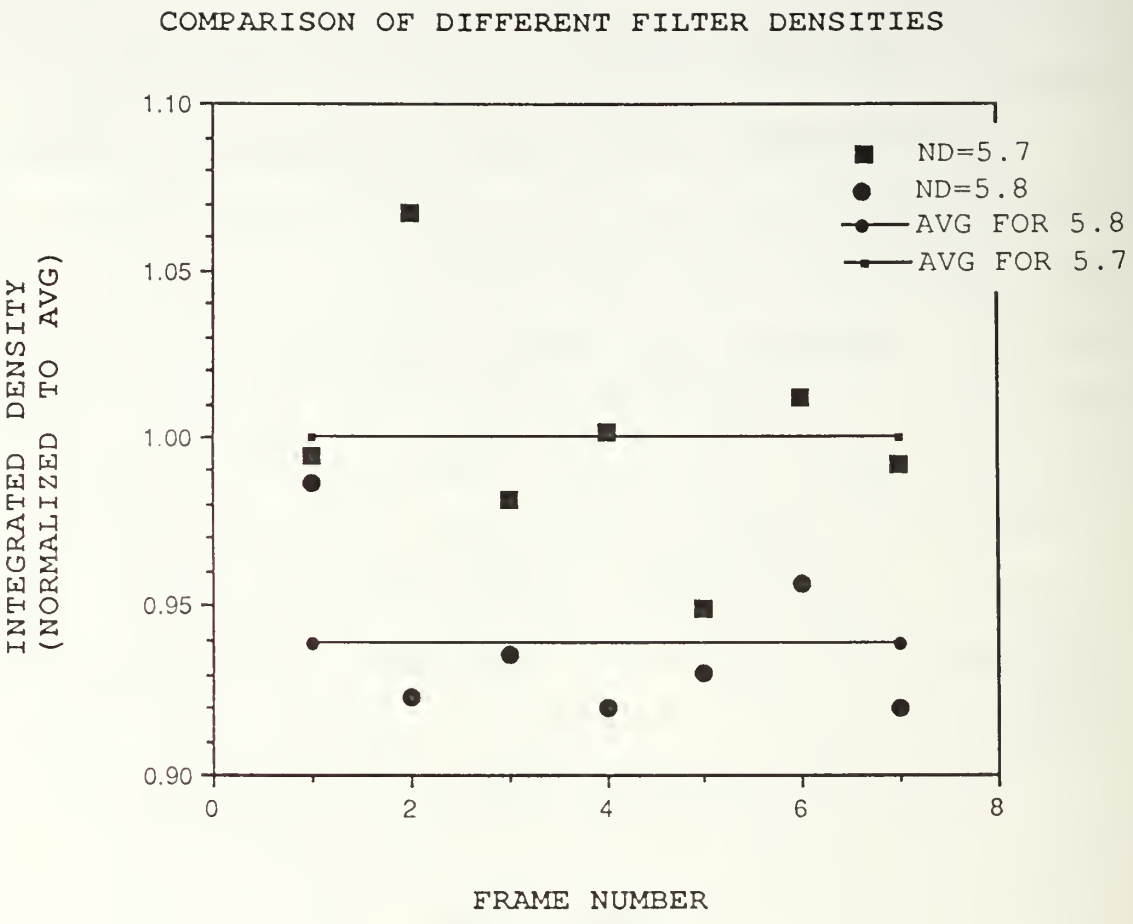

Figure 29: Comparison of integrated density of laser beam image for two different optical densities. Note that increasing the optical density causes a decrease in the integrated density. All values are normalized to the average for the 5.7 case (SITCAM).

reducing this fluctuation were directed to the Image 1.14 software program. Two functions from the Image 1.14 program were examined: the Subtract function, and the Average Frames function.

The Subtraction function allows the user to subtract one image from another. A blank background image was subtracted from another image which had a laser beam spot. The intention was to eliminate background effects, and highlight the image of the beam spot. The integrated density of several images with background subtracted was calculated, with the results shown in Figure 30. Wide variations in integrated density values are still evident.

Another image processing function from Image 1.14 is the Average Frames function. The user can select between eight and 100 frames to be averaged in producing an image. Figure 31 shows the results from using the Vidicon TV camera to average eight frames. The variation level in integrated density between images is still a significant ten percent. Because the variation in integrated density between images was not reduced by the Average Frames function, a final idea was investigated. Instead of viewing a laser beam spot in the TV camera, the Vidicon camera was used to view a still image of the lab equipment used in the experimental setup. Figure 32 shows the result of viewing a still image rather

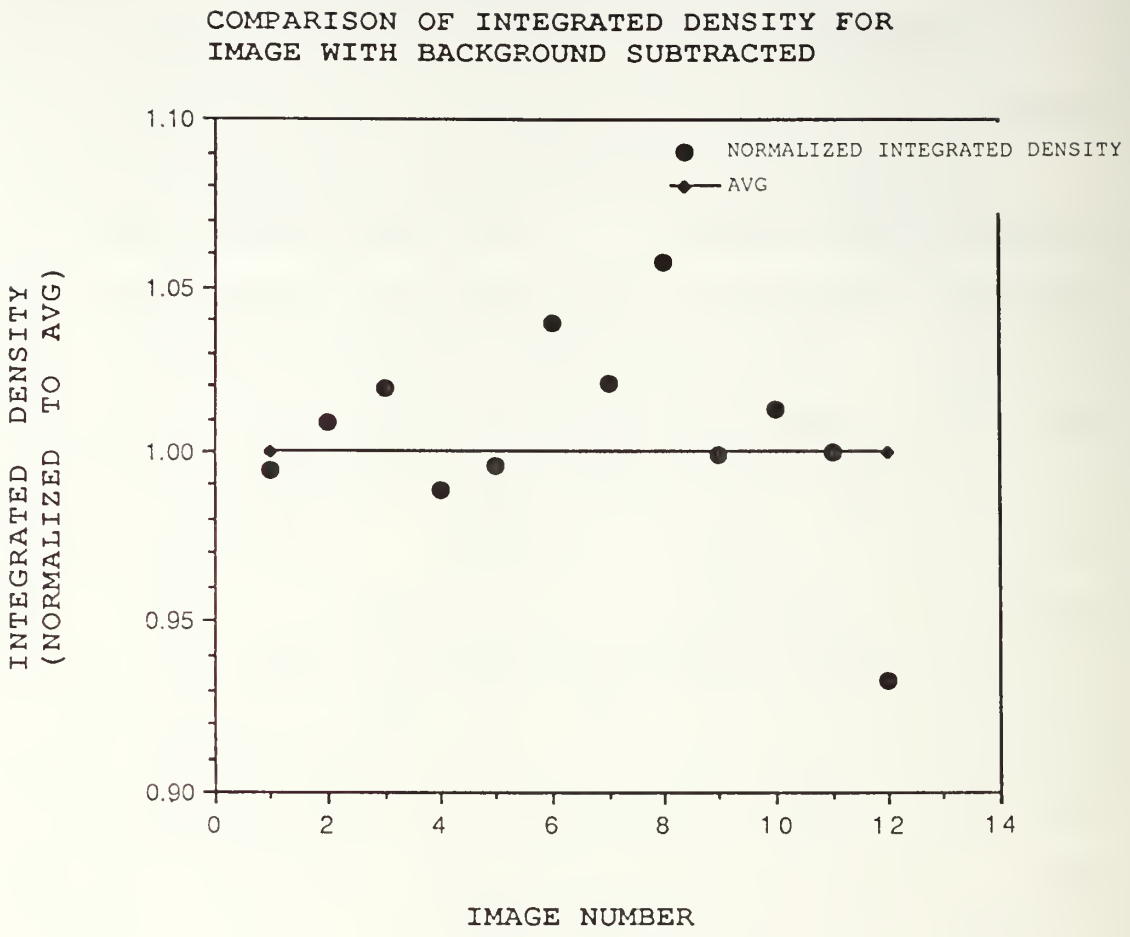

Figure 30: Comparison of integrated density for several images of a laser spot with the background subtracted. Note the significant variations in the normalized integrated density values (SITCAM).

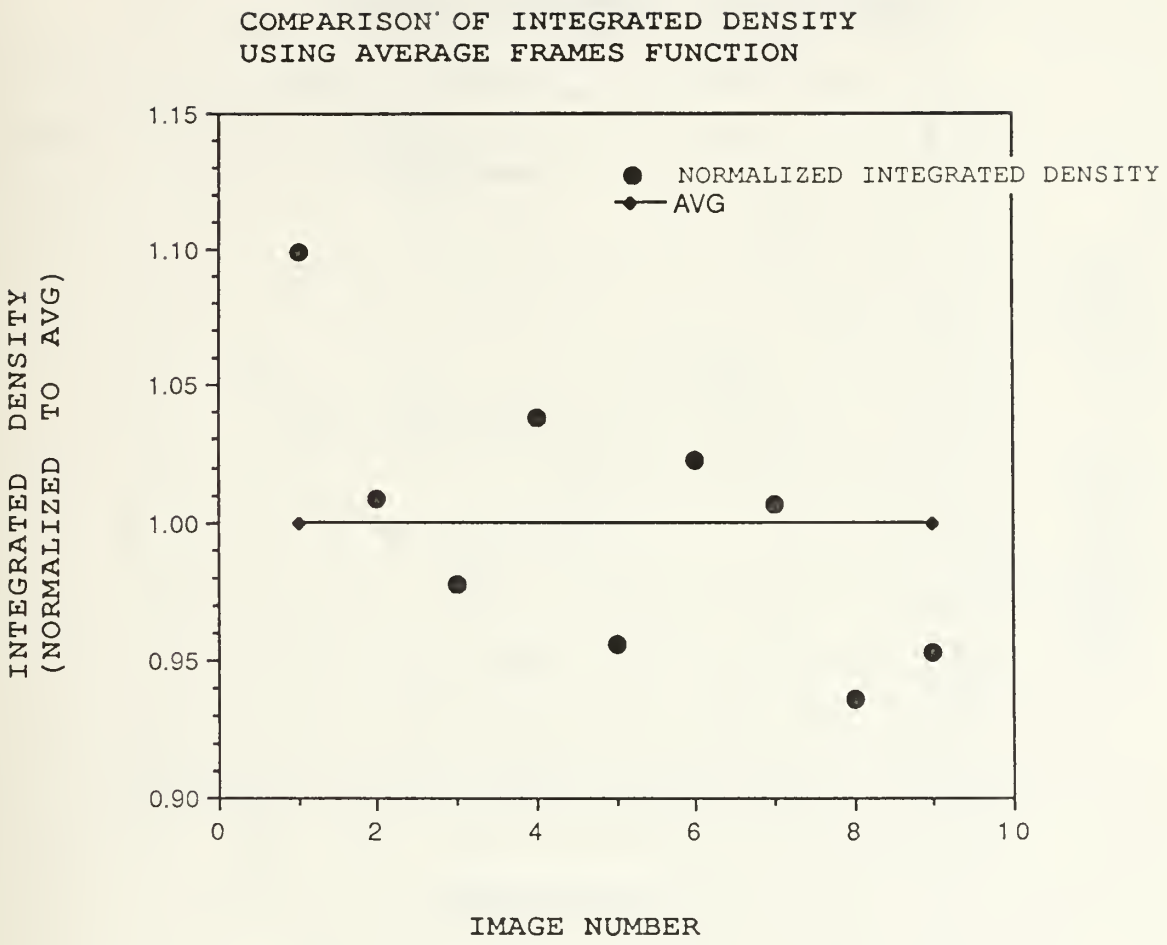

Figure 31: Comparison of integrated density for several images of a laser spot taken using the Average Frames function. Note the variation in values for integrated density (Vidicon).

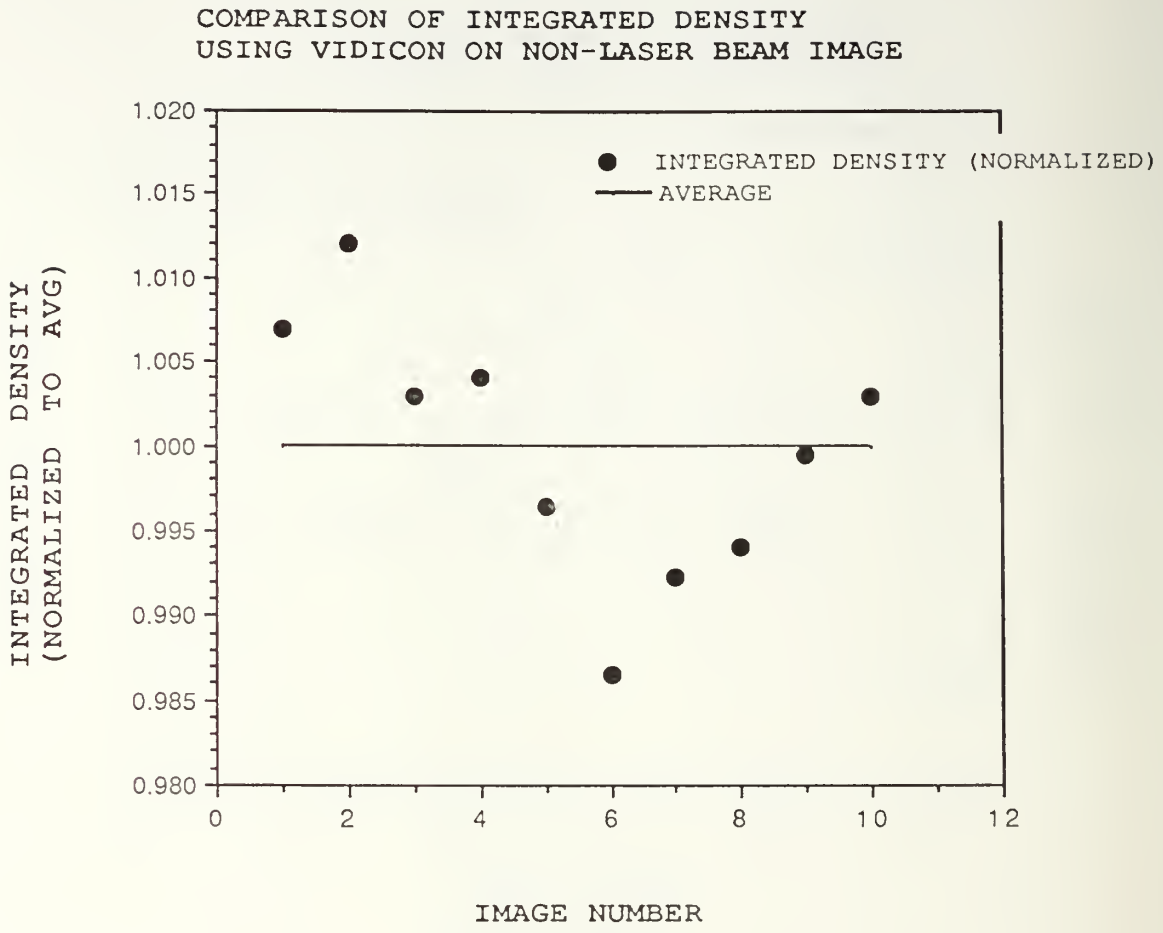

Figure 32: Comparison of integrated density for several images taken of a still image. The Vidion camera was used along with the Average Frames function. Notice the very small variations in integrated density seen above in comparison with Figure 30 (note the change in vertical scaling). (Vidicon)

than a laser beam image. Note that the vertical scaling is significantly reduced from previous graphs.

The Average Frame function produced an integrated density value which showed a 3% variation over the ten images. A 3% variation contrasts sharply with the previous figures presented which had 10 to 15% variations. The utility of the Average Frame function can be seen. The laser beam image gave large variations in the integrated density, but a still video image gave much smaller variations. The laser was assumed to be a constant image light source, but this was an incorrect assumption.

Upon further investigation of the result shown above (3% variation in intensity), it was found that the laser being used was not mode-locked, i.e., its modes are unstable. As a consequence, the polarization of the laser is changing with time. When this laser is used in an experimental setup with two reflections, one particular linear polarization state is preferential over another. The intensity, as observed by the camera, is changing with time. To test this conclusion, a polarizing filter was placed between the laser and the two reflections of the setup. The result was a dramatic, sharply varying intensity of the laser beam image seen by the TV camera. Several images were taken of the laser beam pointing directly into the SITCAM with no reflections. The results are shown in Figure 33, with the

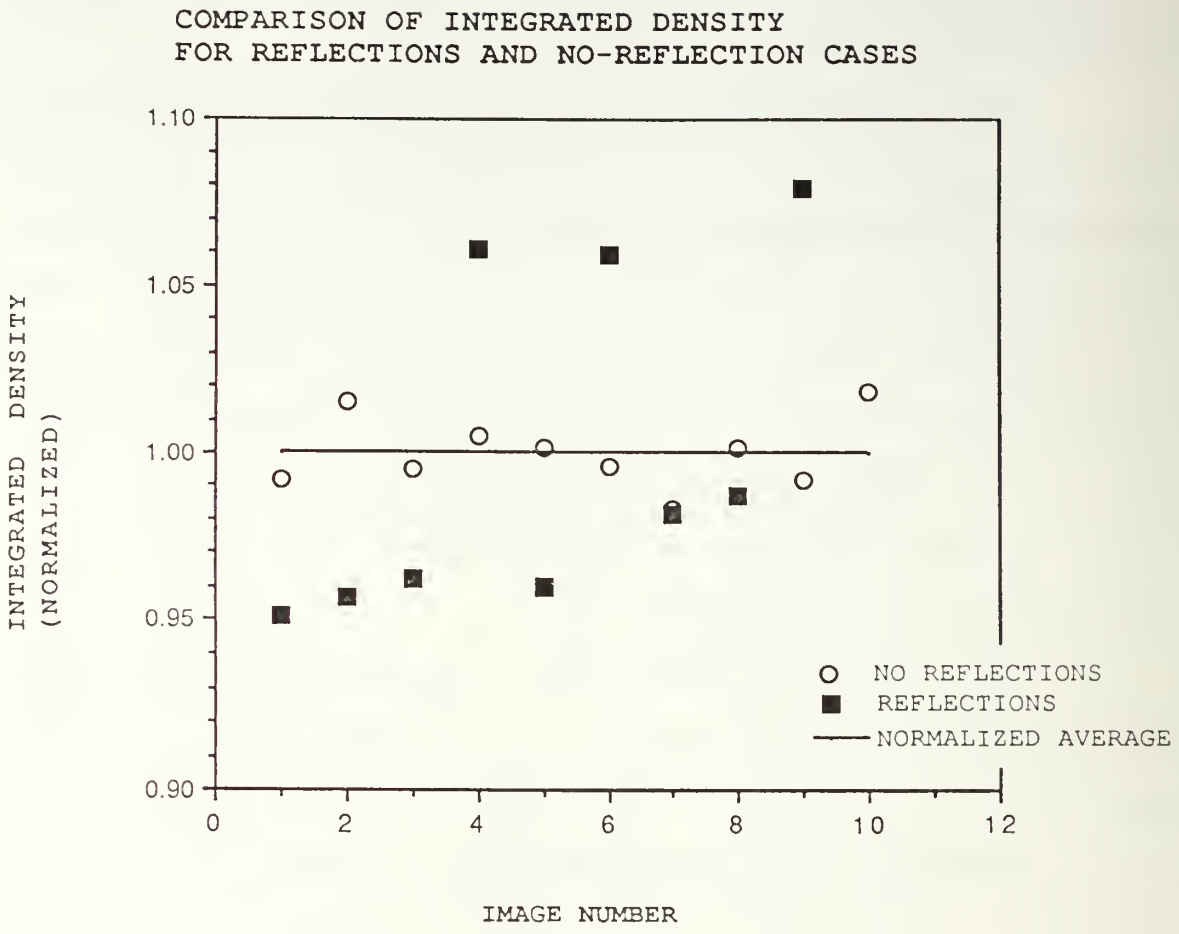

Figure 33: Comparison of the Integrated Density function for the case of laser beam image with reflections and no reflections. Reflections case means that laser beam reflects off two mirrors,no reflections case means that laser beam goes directly into TV camera. Note significant decrease for no reflections case. (SITCAM)

previous results of Figure 24 superimposed. Figure 24 was taken with the same camera under the same conditions, but with the two mirror reflections. Note the large decrease in the variation of integrated density between images for the case of no reflections.

The important point to note is that the polarization of the laser beam is changing as the beam goes through the setup and reflects off the two mirrors. The result is that the intensity seen by the TV camera is changing with time, not constant, as assumed.

6. Experimental Pitfalls and Lessons Learned

Experimental work involves solving problems not previously encountered, with much time spent finding solutions that may appear obvious after the fact. As a footnote to this chapter on experimental results, several experimental pitfalls and lessons learned will be discussed in this section. It must be emphasized that this is a composite list of methods not to be used and lessons learned after considerable time had been invested. By grouping these pitfalls and problems in one section, it is hoped that future experimental work in OTR will be able to benefit from this work.

Chapter III included a procedure to capture images. Two points are worth mentioning regarding the image capturing process. The method presented earlier included inverting

images after they were captured in order to obtain three dimensional plots which appear similar to Figure 9. When continually inverting images, it is possible that the background will retain the image previously captured. The reason for this is unclear, but the problem can be solved by using the Fill command to fill the background with the color black. A good image can then be captured and inverted.

Another method to solve the problem just described was investigated, and shown to be a method not to be used. The Save Blank Field command under the Analysis menu will save a medium brightness blank field used to correct for nonuniform illumination and nonuniform response of the video camera. It is selected while in the live video mode, and then an image is captured. The resulting image gave a three-dimensional plot which was distorted, appearing half up, half down, or not appearing at all. No useful results were obtained using the Save Blank Field option.

The problem of saturation of the TV camera was mentioned. Saturating the TV camera produces the flat-topped beam profile which is of no use. Much time was spent examining images which were saturated. While doing experimental work and examining several parameters, a continual effort should be made to prevent saturation so that results are useful.

Background noise was also discussed as a source of error. The signals between the computer, camera, camera control unit, and auxiliary monitor must be vertically synchronized. By putting these four electronic components on the same 60 Hz power source, gross background noise was eliminated.

The Subtraction function was mentioned as a method to reduce background effects. Both the QuickCapture and Image 1.14 programs have the Subtract option. The QuickCapture program produced an image which only carried video information on every fifth line so it was not useful. A solution to this problem was not found for QuickCapture. However, Image 1.14 produced a useful image, so it was used to subtract images instead of QuickCapture.

The Average Frames function was shown to be very useful for reducing the variation in integrated density values between several images. The TV camera used to obtain this result was the Vidicon, not the SITCAM. Initial efforts of this work were directed toward understanding the capabilities of the SITCAM because it would have been the camera used to view OTR images from the LINAC. The Average Frames function did not work with the SITCAM, though, because the image continually moved around on the screen. The image would jump between two spots on the screen about 20 pixels apart, and also horizontally and vertically by a single pixel. The auxiliary TV monitor produced a steady image

which did not move around on its screen. It was found that there is a problem of signal synchronization between the SITCAM and the frame grabber board. The frame grabber board requires a standard RS-170 signal, and the signal from the SITCAM should also be RS-170 [Ref. 16]. A synchronization board had been added to the camera control unit of the SITCAM to create a standard RS-170 signal, so the exact reasons for the cause of the synchronization mismatch is still unclear. Since the signal coming out of the SITCAM digitizer is producing a good signal on an auxiliary monitor, it should also produce a steady image on the Macintosh computer in the live video mode, but this was not the case. Further efforts to resolve the moving image problem on the Macintosh screen are required. Individual images can be captured and quantitative results can be produced. The ability to average several frames before capturing images, however, is not possible with the SITCAM because the image is not steady on the screen.

C. CONCLUSIONS

The experimental setup described in this work is an integrated system to observe and measure optical transition radiation. Useful qualitative results are quickly produced with this setup. In addition, the experimental setup and software packages described is a quantitative system ready for use with an electron beam. The capability to measure

optical transition radiation from an electron beam has been shown.

The experimental setup described in this work will measure optical transition radiation effectively with an angular resolution of 600 microradians. The frame grabber board and accompanying software (Image 1.14 and QuickCapture) are designed to obtain images quickly and easily. The basic optical design facilitates an alignment procedure which will accurately couple the electron beam from a linear accelerator to the optical axis of the experimental setup. The two focal planes of interest can be found and maintained while running the experiment.

The software manipulation has been extensively described, and its advantages and disadvantages have been detailed. Capturing images is an easy process, and a three dimensional plot can quickly produce useful qualitative results. One dimensional line scans (profile plots) are very useful for analyzing OTR images. The Average Frames function was found to work quite well with the Vidicon which produced an image that did not move around on the computer screen. The Integrated Density function exhibits a capability to measure relative intensity. A software option to subtract out the background is available to the user as a method to reduce variations between images. The three dimensional plots

produced by Image 1.14 are a very useful qualitative result in quickly determining beam profiles.

Individual pixel variations in intensity were commonly ±1 unit, and at most ± 2 intensity units on a 256 unit scale, an error of only ±1%. When the SITCAM TV camera was used, the image on the Macintosh PC screen continually moved around on the computer screen, disallowing the Average Frames function. The orientation and positioning of neutral density filters is critical, and varying either of these parameters can significantly affect one's results. Difficulties with excessive background noise fluctuations were encountered and corrected by using a common power source to provide vertical synchronization.

D. RECOMMENDATIONS

Recommendation for further work in this are include: (1) eliminating the movement of the beam spot within the image on the computer screen, (2) developing a data file of the digitized image for the purposes of user designed data analysis, and (3) investigating the capability to accurately measure absolute intensity of the OTR pattern.

APPENDIX A. OPTICAL TRANSITION RADIATION THEORY

Transition radiation is produced whenever a charged particle moving uniformly in a straight line crosses the interface between two media with different dielectric constants, such as from a vacuum to a metal. The radiation spectrum produced is continuous, ranging from x-rays to microwaves. In introducing the concept in 1944, Frank and Ginsburg noted that the intensity, polarization, and angular distribution of the radiation depend on the dielectric properties of the two media [Ref. 1].

Transition radiation (TR) can be thought of as a collapsing dipole, i.e., an electron and its image charge positron moving directly toward each other, as seen in the Figure A1 below [Ref. 17]:

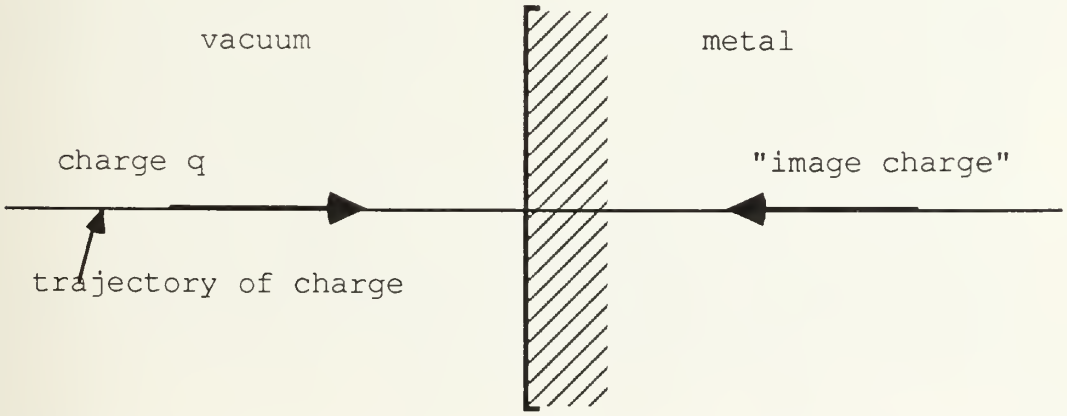

Figure A1: Collapsing dipole model of OTR.

When the electron hits the surface of the second medium, it annihilates with its image charge positron, producing a cone-shaped radiation pattern in the forward and backward directions.

The resulting intensity for a particle of charge e moving with velocity v is

$$\frac{dI}{d\omega d\Omega} = \frac{e^2 \beta^2 \sin^2\theta}{\pi^2 c [1- \beta^2 \cos^2\theta]^2} \qquad \text{(Eqn. 1)}$$

where $d\Omega$ is the solid angle about θ, the angle of observation measured from the normal to the surface, and $\beta = v/c$, with c the velocity of light [Ref. 18]. It can be easily shown that the maximum intensity occurs at the angle $\theta_p \approx 1/\gamma$, where $\gamma = E/mc^2$. E is the total relativistic particle energy, mc^2 is the particle rest mass energy, and γ is the Lorentz factor. The equation listed above for the intensity of the produced radiation assumes the velocity of the electron is normal to the surface of the medium. In an experimental setup, however, tilting the interface at a 45 degree angle to the electron beam permits viewing the backward TR at an angle perpendicular to the electron beam line, as shown below in Figure A2.

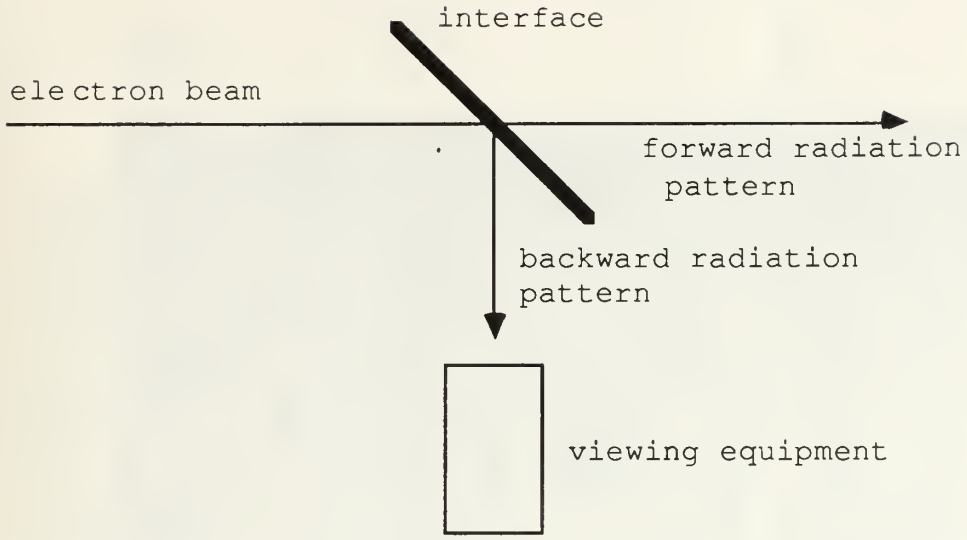

Figure A2: Backward transition radiation can be viewed by orienting OTR interface at 45° to electron beam.

where the backward radiation light is peaked at an angle 90° $\pm\theta_p$ from the electron beam axis. In other words, the light cone is centered around the angle of specular reflection.

Figure A-3 shows a schematic OTR intensity profile. This is a one-dimensional trace across the OTR pattern, and gives the charateristic double-hump apppearance. Note that the maximum intensity occurs at an angle of $\theta_p \approx 1/\gamma$. Also note that the peak intensity is proportional to γ^2.

Finally, Figure A-4 is a picture of an OTR image from a past experiment conducted at the National Bureau of Standards accelerator in Gaithersburg, Maryland [Ref. 10]. Note the donut shape of the beam profile, and also the double ring effect. The double ring is an interference effect. The

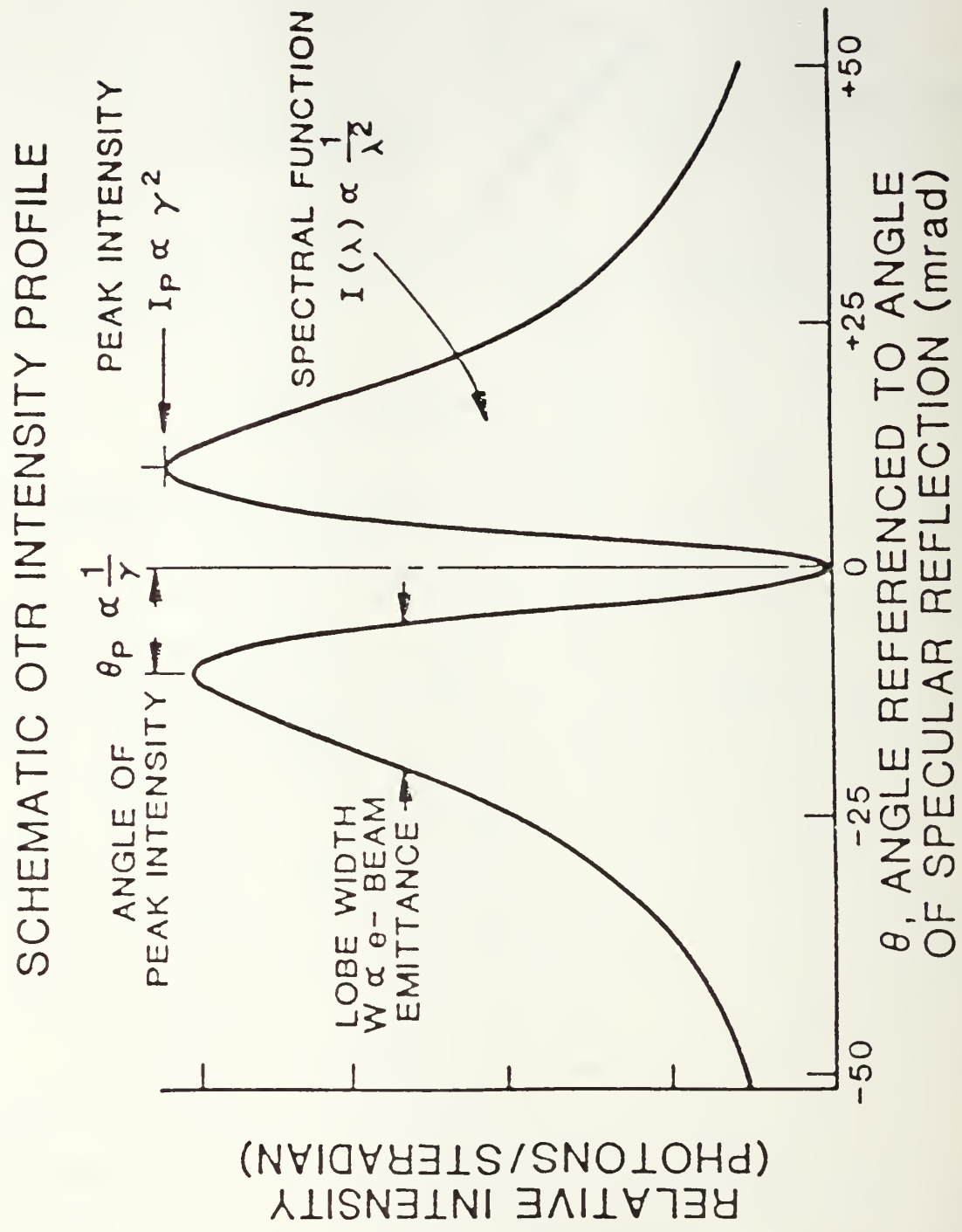

Figure A3: Schematic OTR intensity profile. Note angle of peak intensity is $1/(\gamma)$ and peak intensity is proportional to γ^2. [Ref. 19]

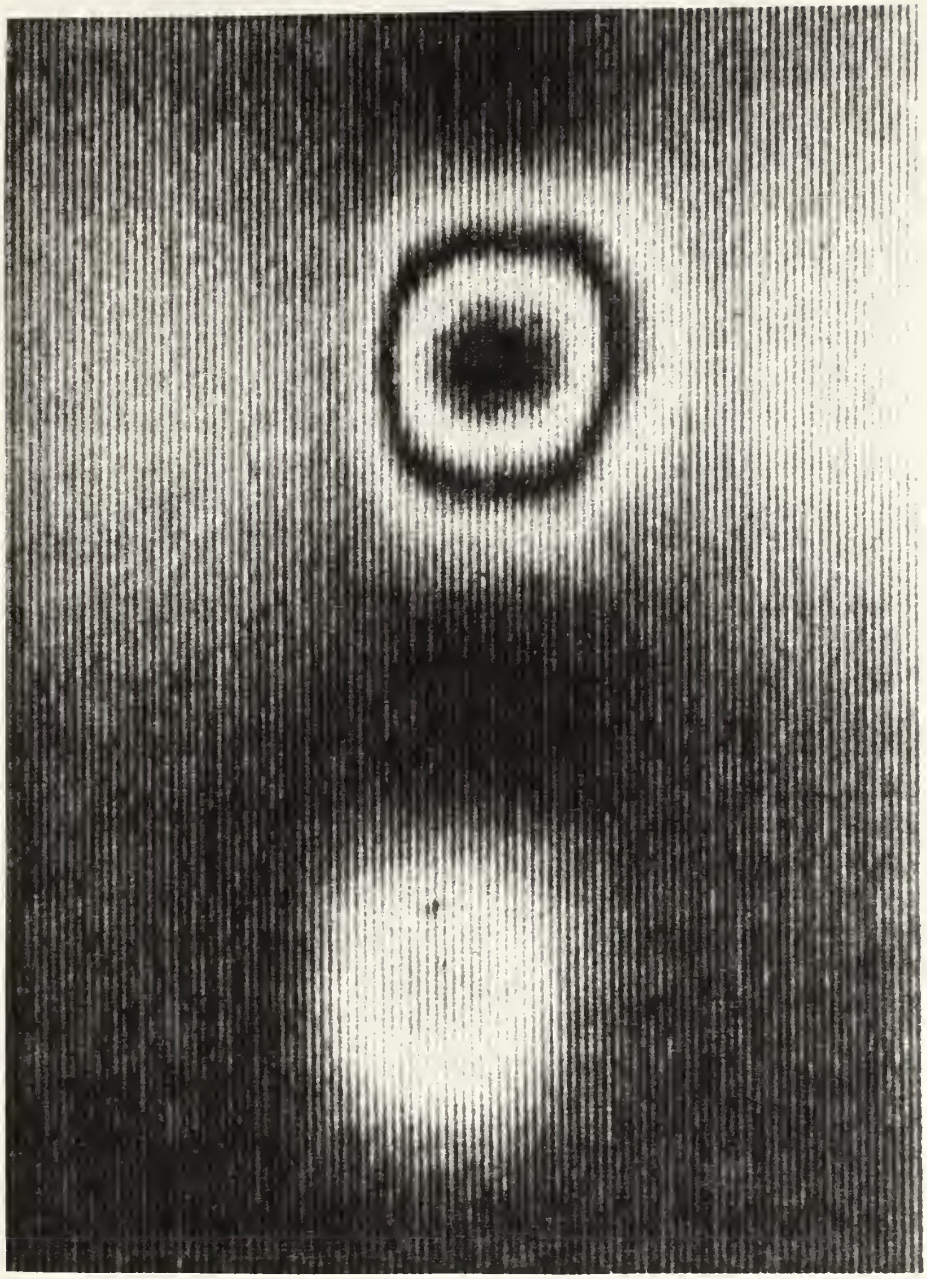

Figure A4: Photograph of OTR image from past experiment conducted at National Bureau of Standards, Gaithersburg, Md. [Ref. 10]

washed out image at the bottom of the picture is a secondary reflection and is not useful.

APPENDIX B. LINAC CHARACTERISTICS

The linear accelerator in use at the Naval Postgraduate School is a radio-frequency, traveling microwave type of machine. It consists of three ten-foot accelerator sections, and each is powered by its own klystron amplifier which delivers up to 21 megawatts peak power. The RF pulse length is 3.5 microseconds, and 120 pulses are formed each second. The electrons are injected from a thermionic emission gun at 80 kilovolts, exiting at a maximum energy of 100 MeV. The average electron current is slightly less than 1 microamp. The operating frequency is 2.856 GHz, which puts it in the S-band. Operating energies range from 15 MeV to 100 MeV. The LINAC at the Naval Postgraduate School is shown in Figure B1.

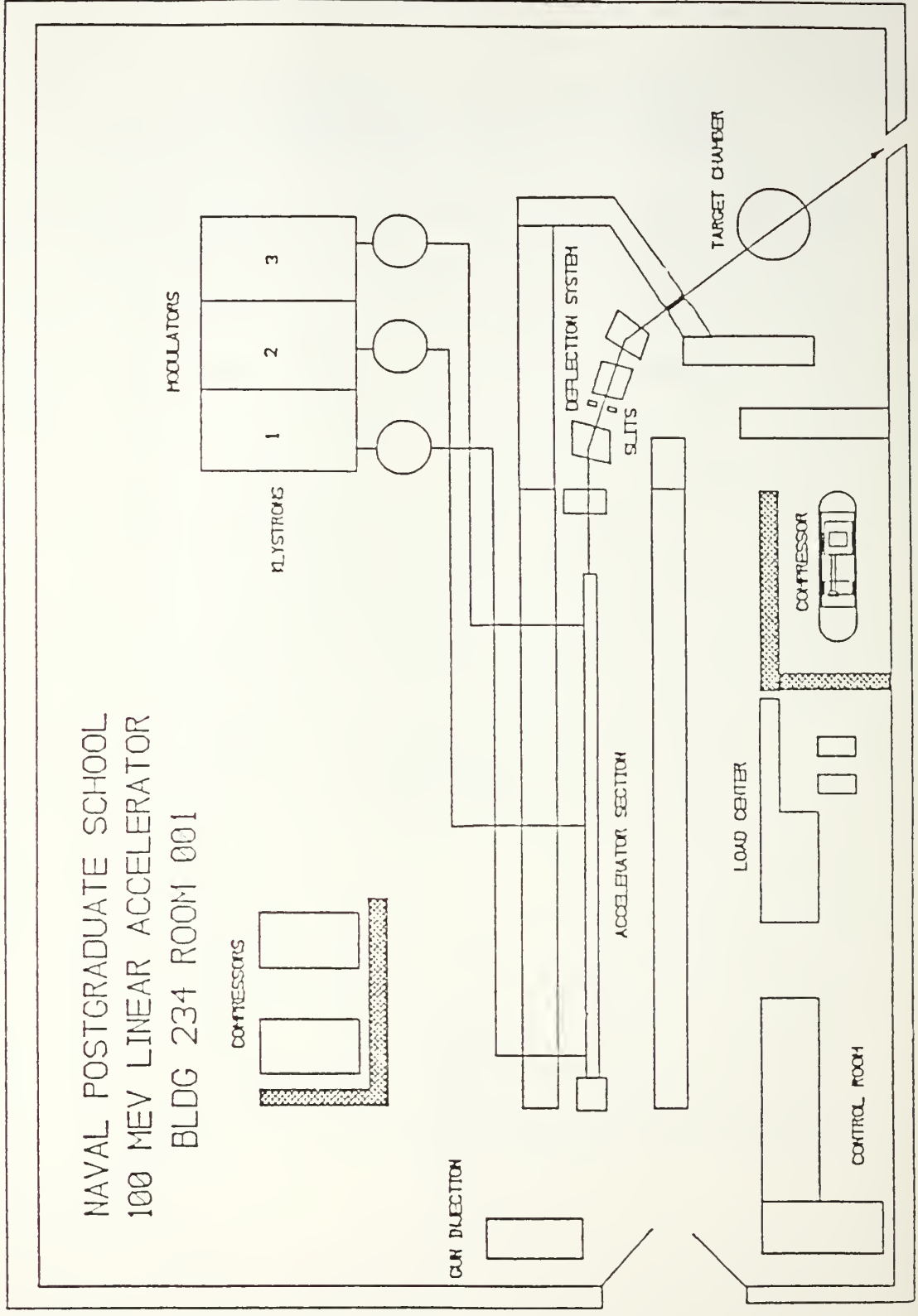

Figure B1: Equipment layout at the LINAC, NPS, Monterey, CA.

APPENDIX C. EQUIPMENT LISTING

PART NUMBER; NAME; FUNCTION.

Manufacturer

Canon

200mm/1:2.8; Camera lens; focuses light pattern.

Newport Corporation

20Z20BD.1; 20th wave zerodur mirror, 2"; reflects light.

10Z20BD.1; 20th wave zerodur mirror, 1"; reflects light.

LS-35; 3' X 5' optical breadboard; for mounting components.

VPH-3; 3" rod holder; vertical post for mounting components.

VPH-4; 4" rod holder; vertical post for mounting components.

SP-3; 3" support post; for mounting components.

P-1, P-5; fixed height post; for mounting components.

MSP-1.5; 1,5" micro-support post; for mounting components.

MPH-2; 2" micro-post holder; hold micro post.

C-1; rod collar; maintains post height.

MPC; micro post collar; maintains post height.

MT-X; microtranslator stage; 1/4" travel stage.

MRL-3; micro optical rail; holds components to table.

MM-2; 2" square mirror mount; holds mirror.

LH2-T; simple lens holder; holds 2" diameter lens.

FH-2; filter holder; holds neutral density filters.

ID-1.0; iris diaphragm; aperture to control emitted light.

LM-2; lens mount; holds 2" diameter lens.

280; lab jack; large lab jack for 3" to 6" height control.

270; lab jack; smaller lab jack, 2" to 4" height control.

CL-4; tie-down clamp; all-purpose clamp.

360-90; angle bracket; sliding bracket for unusual mountings.

B-1, B-2; sliding base; provides mounting base.

BP-5; base plate; provides mounting base

400; dual-axis translation stage; 0.5" travel in 2 directions.

481; rotary stage; for rotary motion.

430-1; translation stage; 1" travel in one direction.

CLMK-B2; lens holder; holds 2" diameter 200mm Canon lens.

SP-6; support post; 6" long post for holding components.

MB-2; magnetic base; magnetic holder for components.

370; rod/clamp assembly; rod and clamp for holding laser.

812; laser mount; two-axis control mount for laser.

U-1301; laser; class IIIA, 1 milliwatt Helium-Neon laser.

Oriel Corporation

11512; large rail; 24" X 4" optical rail for mounting components.

11522; standard rail; 24" X 2" optical rail, holds components.

11601; large rail carrier; 5" square carrier mounts onto rail.

11621; standard carrier; 3" X 3.5" carrier, mounts onto rail.

11641; narrow carrier; 3.25" X 2" carrier, provides stable base.

12055; tilt table; table tilts in horizontal plane in 2 axes.

12312; standard rod; 2" long rod.

12330; standard rod; 4" long rod.

12350; standard rod; 6" long rod.

14421; stable rod holder; 2" high rod holder.

14432; stable rod holder; 4" high rod holder.

14423; stable rod holder; 6" high rod holder.

12510; rod collar; for fixing rod height.

40780; plano-convex lens; 2" diameter lens, focal length of 100mm.

50350; neutral density filter, 1.0; reduces light to 10%.

50360; neutral density filter, 2.0; reduces light to 1%.

50370; neutral density filter, 3.0; reduces light to 0.1%.

27340; linear visible polarizer; 2" diameter, polarizes light.

14230; optical clamp; for holding optical components.

13872; 22" rigid mount; legs for holding optical breadboard.

18011*; Encoder Mike Controller; for controlling motorized stages.

13048*; 360^{o} motorized rotary stage; for precise rotary motion.

16338*; 2" motorized translation stage; for precise linear motion.

18212-1-1200*; electrical cord; connects motorized components with Encoder Mike Controller.

Ealing Electro-Optics, Inc.

2668P74; sector star target; for focusing light.

228437; electronic shutter; opens/closes to admit light.

228460; shutter mount; for holding shutter.

Process Physics, Inc.

C6C-0800*; six-way vacuum chamber; holds OTR mirror.

HTE, Inc.

50054*; standard 8" Conflat flange; for six-way chamber.

50360; nut, bolt, and washer set; 5/16-24 X 2 1/4.

50329; nut, bolt, and washer set; 5/16-24 X 1 3/4.

Duniway Stockroom Corp.

VP-800-600*; glass viewport, 6" O.D., 8" flange O.D.; for viewing.

G-800; copper gaskets; 8" flange O.D. for coupling vacuum parts.

Cohu, Inc.

4815-5000; solid-state, monochrome CCD camera; for viewing OTR.

Hamamatsu, Inc.

C1000*; Silicon Intensified Target TV Camera and camera control unit; for viewing OTR.

C1440*; frame memory image analysis system; digitizer for C1000 camera.

* signifies component (or equivalent) has been borrowed from Dr. R.B. Fiorito, Code R41, Naval Surface Warfare Center, Silver Spring, Maryland.

Manufacturer's Addresses and Phone Numbers

Canon lens obtained from Russell's Camera West, 423 Alvarado St, Monterey, CA 93940 (408) 649-0220

Newport Corp., P.O. Box 8020, Fountain Valley, CA 92728-8020 (714) 963-9811

Oriel Corp., 250 Long Beach Blvd., Startford, CT 06497-0872 (203) 377-8282

Ealing Electro-Optics, Inc., 22 Pleasant St., South Natick, MA 01760 (800) 343-4912

Process Physics, Inc., 816 Charcot Ave., San Jose, CA 95131 (800) 752-3535

HTE Inc., 1001 Shary Circle, Concord, CA 94518 (415) 895-9490

Duniway Stickroom Corp., 1600 N. Shoreline Blvd., Mountain View, CA 94043 (415) 969-8811

Cohu, Inc., 5755 Kearny Villa Rd, P.O. Box 85623, San Diego, CA 92138-5523 (619) 277-6700

Hamamtasu Corp., 360 Foothill Road, Box 6910, Bridgewater, NJ 08807-0960 (201) 231-0960

LIST OF REFERENCES

1. Frank, I., and Ginsburg, V., "Radiation of a Uniformly Moving Electron Due to Its Transition From One Medium into Another," Journal of Physics, Vol. IX, No. 5, pp. 353-362, 1945.

2. Wartski, L., et al, "Detection of Optical Transition Radiation and Its Application to Beam Diagnostics," IEEE Transactions in Nuclear Science, Vol. 20, No. 3, pp. 544-548, 1973.

3. Wartski, L., et al, "Thin Films on LINAC Beams as Non-Destructive Devices for Particle Beam Intensity, Profile, Centering, and Energy Monitors," IEEE Transaction in Nuclear Science, Vol. 22, No. 3, pp. 1552-1557, June 1975.

4. Wartski, L., et al, "Interference Phenomenon in Optical Transition Radiation and its Application to Particle Beam Diagnostics and Multiple Scattering Measurements," Journal of Applied Physics, Vol. 46, No. 8, pp. 3644-3653, 1975.

5. Wartski, L., "Study on the Optical Transition Radiation Produced by 30 to 70 Mev Energy Electrons. Application to the Diagnosis of Beams of Charged Particles," Ph.D. Dissertation, The Universite de Paris-Sud, Centre D'Orsay, France, 1976.

6. Fiorito, R.B., et al, "Optical Transition Radiation Diagnostics for Low Emittance, High Energy, Charged Particle Beams," paper presented at the EPAC Proceedings of the European Particle Accelerator Conference, June 7-11, 1988.

7. Iversen, S.G., et al, "Charged Particle Beam Divergence Measurements Using Transition Radiation," IEEE Particle Accelerator Conference, pp. 573-575, March 16-19, 1987.

8. Naval Surface Weapons Center Report TR 84-134, "The Use of Transition Radiationas a Diagnostic for Intense Beams," by D. W. Rule and R. B. Fiorito, July, 1984.

9. Rule, D.W., et al, "Emittance Characterization of Beams Using Transition Radiation," paper presented at SDIO/DARPA/Services Review, Naval Postgraduate School, Monterey, California, 29 September 1987.

10. Maruyama, X.K., et al, "Optical Transition Radiation as a Real-Time, On-Line Diagnostic for Free Electron Laser Systems," paper presented at IXth International Free Electron Laser Conference, Williamsburg, VA, September 1987.

11. Bates Linear Accelerator Center, Massachusetts Institute of Technology, Annual Scientific and Technical Report, 1987-1988, "Accelerator Developments", by Biron, R.D. et al, pp. 205-210, 1988.

12. Hecht, E., Optics, 2d ed., p. 138, Addison Wesley Publishing Co., 1987.

13. Private communication between Dr. Ralph Fiorito, Naval Surface Warfare Center, and author, 23 February 1989.

14. Data Translation, Inc., QuickCapture User Manual, 2d ed., pp. 21-67, August, 1988.

15. Oriel Corporation, Oriel Catalog, Vol. III, p. 4, 1984.

16. Telephone conversation between Mr. Oshiro, Hamamatsu Corporation and the author, 7 December 1989.

17. Ginzburg, V., and Tsytovich, V.N., "Several Problems of the Theory of Transition Radiation and Transition Scattering," Physics Reports, Vol.49, No. 1, p. 6, 1979.

18. Ginzburg,V., "Transition Radiation and Transition Screening," Physica Scripta, Vol. T2/1, p. 182, 1982.

19. Private communication between Dr. Ralph Fiorito, Naval Surface Warfare Center, Dr. Xavier Maruyama, Naval Postgraduate School, and the author, 25 February 1989.

INITIAL DISTRIBUTION LIST

		No. Copies
1.	Defense Technical Information Center Cameron Station Alexandria, VA 22304-6145	2
2.	Library, Code 0142 Naval Postgraduate School Monterey, CA 93943-5002	2
3.	Dr. K. E. Woehler, Code 61Wh Department of Physics Naval Postgraduate School Monterey, CA 93943-51002	1
4.	Professor X. K. Maruyama, Code 61Mx Department of Physics Naval Postgraduate School Monterey, CA 93943-5002	2
5.	Professor J. R. Neighbours, Code 61Nb Department of Physics Naval Postgraduate School Monterey, CA 93943-5002	2
6.	Dr. R. B. Fiorito, Code R41 Naval Surface Warfare Center 10901 New Hampshire Ave. Silver Spring, MD 20903-5000	1
7.	Dr. D. W. Rule, Code R41 Naval Surface Warfare Center 10901 New Hampshire Ave. Silver Spring, MD 20903-5000	1
8.	Dr. M. A. Piestrup Adelphi Technology, Inc. 532 Emerson Street Palo Alto, CA 94301	1
9.	Dr. T. I. Smith HEPL 13 685 Wildwood Lane Palo Alto, CA 94303	1
10.	Dr. R. L. Swent HEPL 13 685 Wildwood Lane Palo Alto, CA 94303	1

11. Lieutenant D. M. Caldwell 1
Naval Postgraduate School SMC 1906
Monterey, CA 93943

12. Dr. D. W. Beck 1
Department of Physics
University of Illinois at Urbana-Champaign
110 W. Green Street
Urbana, IL 61801

13. Mr. D. Synder, Code 61Ds 1
Department of Physics
Naval Postgraduate School
Monterey, CA 93943-5002

14. Mr. H. Rietdyk, Code 61Hr 1
Department of Physics
Naval Postgraduate School
Monterey, CA 93943-5002

15. LT P. K. Dallman 2
186 Cranwood Drive
West Seneca, NY 14224

Thesis
D1436 Dallman
c.1 Establishment of a capability to measure optical transition radiation.